QUASIPARTICLE PROPERTIES IN ALUMINUM

A THEORETICAL CALCULATION OF QUASIPARTICLE PROPERTIES IN ALUMINUM

By

NEIL LLEWELLYN McKAY, B.Sc.

A Thesis
Submitted to the School of Graduate Studies
in Partial Fulfilment of the Requirements
for the Degree
Master of Science

McMaster University
December 1976

MASTER OF SCIENCE (1976)
(Physics)

MCMASTER UNIVERSITY
Hamilton, Ontario

TITLE: A Theoretical Calculation of Quasiparticle Properties in Aluminum

AUTHOR: Neil Llewellyn McKay, B.Sc. (Queen's University)

SUPERVISOR: Professor J. P. Carbotte

NUMBER OF PAGES: v,59

ABSTRACT

Theoretical calculations of the renormalization of the electron mass and the quasiparticle lifetime due to the electron-phonon interaction are performed in aluminum as a function of position on the Fermi surface. The computations are carried out at finite temperature, and, in the case of the relaxation time, for finite energy above the Fermi surface.

We present a formal development of expressions for the mass renormalization parameter and lifetime at finite temperature to second order in the electron-phonon interaction using a perturbation-theory approach, which is mathematically simpler, if less elegant, than the usual Greensfunction method. The behaviour of the resulting integrals is discussed briefly with reference to their numerical evaluation.

Our results for the electron mass renormalization at finite temperature agree qualitatively with the expected variation of the electron wavefunctions on the Fermi surface. In terms of the results, the approximate requirements for experimental observation of the calculated increase in electronic effective mass and its anisotropy are discussed.

A comparison of the calculated temperature dependence of the quasiparticle lifetime with experiment and with other theoretical work has important implications for the accuracy of electron-phonon numerical calculations in the low-frequency region.

ACKNOWLEDGEMENTS

My thanks to my supervisor, Dr. J. P. Carbotte, for his patient encouragement during the course of this enterprise, and for taking a sabbatical in Paris.

I would like gratefully to acknowledge the assistance with the computer of Dr. Dale Ellis, and the money of the National Research Council and the International Nickel Company of Canada Limited.

I particularly thank Mrs. Helen Kennelly for her rapid and cheerful typing of this thing.

TABLE OF CONTENTS

CHAPTER I

INTRODUCTION

In a normal metal in equilibrium, the interaction between conduction electrons near the Fermi surface and the vibrational modes of the crystal leads to a shift in energy of the electron states, often described as change in the electronic effective mass, and scatters electrons between states near the Fermi surface with a characteristic relaxation time. Grimvall (1968) noticed that this electron-phonon interaction was distinguished from other contributions to the effective mass observed in cyclotron resonance by a significant dependence on temperature. Using Greens function methods, he calculated the temperature-dependent electron mass renormalization parameter λ in an Einstein model and in a more detailed model of sodium. In 1969 Allen and Cohen calculated λ(T) in an isotropic model for several metals, and found reasonable agreement with the simultaneous experiments of Sabo on zinc. Recent detailed calculations by Leung (1974) of direction-dependent frequency distributions characterizing the electron-phonon in aluminum have made possible the present calculation of λ as a function of temperature and of position on the Fermi surface. We also calculate the lifetime τ, which is closely related theoretically and experimentally, as a function of temperature, energy, and direction. Aluminum is of interest largely for being a superconductor which, as a polyvalent metal, is only one step more difficult to deal with theoretically than the alkalis.

We begin in Chapter II by presenting the model of a metal in which we shall work and develop the fundamental expression describing the electron-phonon interaction. Essentially, this chapter is a review of methods commonly used in the field. Features and limitations of the model are discussed with a view to justifying the approximations of the subsequent theoretical development.

In the third chapter the expressions for λ and τ are derived, using an ordinary perturbation-theory approach for its simplicity. Wilkins (1968) presents such a perturbation-theory development of an expression for λ at zero temperature, and in an appendix extends it to finite temperature with intuitive arguments. Here we present a formal development at finite temperature of equations for λ and τ.

Our results are presented in the next chapter. The orientation of the coordinates describing positions on the Fermi surface is explained in somewhat laborious detail, but this should be an aid in correlating our points with the invariably different systems of other installations. Numerical procedures and difficulties are described briefly. We present our results in tables and graphs and discuss their behaviour. The calculated lifetimes of Tomlinson and Carbotte (1976) and those measured experimentally by Doezema and

Wegehaupt (1975) are compared with the present calculations.

Chapter V concludes with a discussion of the implications of these results to experiments and theoretical calculations.

CHAPTER II

ELECTRONS IN A LATTICE

2.1 The Pseudopotential Method

We are concerned in this work with the effect of the crystal lattice upon conduction electrons, and more specifically with the electron-phonon interaction. Although the ion lattice enters into this problem in a fundamental way, we may use the Born-Oppenheimer theorem to focus our attention on the electrons, which to a good approximation obey a Schrödinger equation involving the ion coordinates only as parameters in the potential felt by an electron (Ziman, 1972). Describing the electron-electron interactions by including a self-consistent interaction energy in the potential, we arrive at a single-electron equation,

$$(T + V(\underline{r}))\psi(\underline{r}) = \varepsilon\psi(\underline{r}) \tag{2.1}$$

where $T \equiv -\frac{\hbar^2}{2m}\nabla^2$ is the kinetic energy operator, $V(\underline{r})$ is the self-consistent potential seen by an electron at $\underline{r}$, and $\psi(\underline{r})$ is a single-electron wavefunction with energy eigenvalue ε.

The Hamiltonian in (2-1) is not time-independent. The lattice is free to vibrate, and the potential $V(\underline{r})$ follows the motion of the ions. This time-varying part in the Hamiltonian, the electron-phonon interaction, will be discussed in subsequent chapters in terms of its effect on the wavefunctions obtained as solutions to the static part of (2.1). In the remainder of this section we shall review the method of pseudopotentials (Harrison, 1966) which allows the use of familiar and convenient techniques for extracting information of physical interest from (2.1).

We consider a pure metal with the ions at their equilibrium positions on a perfect lattice. Taking the potential $V(\underline{r})$ to be a sum of (identical) single-ion potentials $v(\underline{r})$, we write (2.1) as

$$[T + \sum_{\ell} v(\underline{r}-\underline{R}_{\ell}^{o})]\psi(\underline{r}) = \varepsilon\psi(\underline{r}) \tag{2.2}$$

for the ions fixed to their equilibrium positions R_{ℓ}^{o}. This equation describes all the electrons. For non-transition metals such as aluminum, the core electrons are confined to a region much less than the size of the unit cell. To a good approximation the core wavefunctions do not overlap into the regions where the potential due to neighbouring ions is large, and are essentially unchanged from the wavefunctions of the free ion. The conduction electron states are spread through the crystal, and their qualitative behaviour is strongly influenced by the distribution of the points $\underline{R}_{\ell}^{o}$ about which the potentials are centred.

The translational symmetry of the Hamiltonian in (2.2) requires that the solutions have the Bloch form (Ziman, 1972)

$$\psi_{\underline{k}}(\underline{r}) = \frac{1}{\Omega^{1/2}} u_{\underline{k}}(\underline{r}) e^{i\underline{k}\cdot\underline{r}} \tag{2.3}$$

where $u_{\underline{k}}(\underline{r})$ has the translational symmetry of the crystal; that is

$$u_{\underline{k}}(\underline{r} + \underline{R}_{\ell}^{o}) = u_{\underline{k}}(\underline{r}) \ .$$

The crystal volume Ω is explicitly included in (2.3) for normalization. We apply periodic boundary conditions on the crystal to specify the allowed values of wavevector $\underline{k}$.

The periodicity of $u_{\underline{k}}(\underline{r})$ demands that it be expressable as the Fourier sum

$$u_{\underline{k}}(\underline{r}) = \sum_{n} C_n(\underline{k}) e^{i\underline{\kappa}_n \cdot \underline{r}} \tag{2.4}$$

where the sum is over reciprocal lattice vectors $\underline{\kappa}_n$. Putting (2.3) and (2.4) together gives, finally,

$$|\psi_{\underline{k}}> = \sum_{n} C_n(\underline{k}) |\underline{k} + \underline{\kappa}_n> \tag{2.5}$$

We have gone to Dirac notation with the substitution

$$\frac{e^{i\underline{p}\cdot\underline{r}}}{\Omega^{1/2}} \rightarrow |\underline{p}> .$$

Solving the Schrödinger equation (2.2) is equivalent to finding the expansion coefficients $C_n(\underline{k})$ in (2.5).

An approximate solution could be generated by truncating (2.5) after a finite number of terms, substituting into (2.2), and solving the resulting matrix equation for the C_n's and the eigenvalues ε. However, the number of terms required for an accurate description of the true wavefunction is large. It would be preferable to begin with a set of basis functions other than simple plane waves, which more nearly approximate the true electronic eigenstates.

Since the conduction-band states must be orthogonal to the core states, Herring (1940) suggested the use of orthogonalized plane waves (OPW's), defined by

$$|OPW_{\underline{k}}\rangle = |\underline{k}\rangle - \sum_{\alpha} |\alpha\rangle\langle\alpha|\underline{k}\rangle \tag{2.6}$$

where the sum is over all core states $|\alpha\rangle$. The OPW is just a plane wave minus its projection on the core states, and has the symmetry demanded by (2.3), since the core states do. Expanding the electron wavefunction in OPW's gives

$$\begin{aligned}|\psi_{\underline{k}}\rangle &= \sum_{n} a_n(\underline{k})\,|OPW_{\underline{k}+\underline{\kappa}_n}\rangle \\ &\equiv \sum_{n} a_n(\underline{k})\{|\underline{k}+\underline{\kappa}_n\rangle - \sum_{\alpha} |\alpha\rangle\langle\alpha|\underline{k}+\underline{\kappa}_n\rangle\} .\end{aligned} \tag{2.7}$$

The core states are eigenstates of the Hamiltonian with energies we shall denote by ε_α. Substituting (2.7) into the Schrödinger equation (2.2), we obtain for a conduction electron in state $|\psi_{\underline{k}}\rangle$,

$$\begin{aligned}&\sum_{n} a_n(\underline{k})\{(T + \sum_{\ell} v(\underline{r}-\underline{R}_\ell^o))\,|\underline{k}+\underline{\kappa}_n\rangle - \sum_{\alpha} \varepsilon_\alpha|\alpha\rangle\langle\alpha|\underline{k}+\underline{\kappa}_n\rangle\} \\ &\qquad = \varepsilon_{\underline{k}} \sum_{n} a_n(\underline{k})\{|\underline{k}+\underline{\kappa}_n\rangle - \sum_{\alpha} |\alpha\rangle\langle\alpha|\underline{k}+\underline{\kappa}_n\rangle\} .\end{aligned} \tag{2.8}$$

Following Harrison (1966) we take all the core state terms to the left side and with a little rearrangement write

$$\begin{aligned}&\sum_{n} a_n(\underline{k})\{T + \sum_{\ell} v(\underline{r}-\underline{R}_\ell^o) + \sum_{\alpha} (\varepsilon_{\underline{k}}-\varepsilon_\alpha)\,|\alpha\rangle\langle\alpha|\}\,|\underline{k}+\underline{\kappa}_n\rangle \\ &\qquad = \varepsilon_{\underline{k}} \sum_{n} a_n(\underline{k})\,|\underline{k}+\underline{\kappa}_n\rangle .\end{aligned} \tag{2.9}$$

We have treated $\sum_{\alpha} |\alpha\rangle\langle\alpha|$ as a projection operator and separated it from the ket $|\underline{k}+\underline{\kappa}_n\rangle$.

Equation (2.9) may be written in a more transparent form. We define the pseudopotential W by

$$W(\underline{r}) = \sum_{\ell} v(\underline{r}-\underline{R}_{\ell}^{o}) + \sum_{\alpha} (\varepsilon_{\underline{k}}-\varepsilon_{\alpha})|\alpha\rangle\langle\alpha| \qquad (2.10)$$

and a corresponding pseudowavefunction $|\phi_{\underline{k}}\rangle$ through the relation

$$|\psi_{\underline{k}}\rangle = |\phi_{\underline{k}}\rangle - \sum_{\alpha} |\alpha\rangle\langle\alpha|\phi_{\underline{k}}\rangle \qquad (2.11)$$

that is,

$$|\phi_{\underline{k}}\rangle = \sum_{n} a_n(\underline{k})|\underline{k}+\underline{\kappa}_n\rangle \qquad (2.12)$$

in the above expressions. (2.9) takes the simple form

$$(T+W)|\phi_{\underline{k}}\rangle = \varepsilon_{\underline{k}}|\phi_{\underline{k}}\rangle \quad . \qquad (2.13)$$

It is not obvious that we have gained by all this, as we have arrived back at a Schrödinger equation with the pseudopotential and pseudowavefunction replacing the true potential and wavefunction. The value of (2.13) in what follows rests on W being much weaker than the true potential, so that it may be treated as a perturbation on a (pseudo) electron gas. This is equivalent to saying that we expect the conduction band wavefunctions to be nearly described by a single, or at worst a few, OPW's. Using (2.13) allows us to work with a small number of plane waves, at the expense of employing a complicated pseudopotential.

From (2.10) it is apparent that W is an operator rather than simply a c-number function, and that it depends explicitly on the energy $\varepsilon_{\underline{k}}$ of the state under consideration. Since we always work at or very near the Fermi energy, the energy dependence is not a problem. More serious is the nonlocal operator nature of W. The form factor $\langle\underline{k}|W|\underline{k}'\rangle$ contains the product $\langle\underline{k}|\alpha\rangle\langle\alpha|\underline{k}'\rangle$, and does not depend only on the momentum transfer $\underline{k}'-\underline{k}$. Model pseudopotentials have been constructed (see, for example, Heine and Abarenkov, 1964) which are local and greatly simplify subsequent computations.

It is necessary to introduce the pseudopotential due to a single ion at the origin,

$$W(\underline{r}) = v(r) + \sum_{\alpha} (\varepsilon_{\underline{k}}-\varepsilon_{\alpha})|\alpha\rangle\langle\alpha| \qquad (2.14)$$

where the sum is now over the core states of the free ion, and to assume that the full pseudopotential is the sum of single-ion pseudopotentials centred about all the ions. This approximation has already been justified for the potential term in (2.10). Under the same assumption that the core wavefunctions are highly localized, the projection operator terms sum in the same way.

2.2 The Electron-Phonon Interaction

We deal in this section with a crystal of N identical ions in a sea of conduction electrons. Each electron interacts with each ion through a weak pseudopotential W. Electron-electron interactions are ignored except for those effects included as screening terms in W. The ions are allowed to oscillate about their equilibrium positions, and following White (1974) an expression is derived for the correction to the many-electron Hamiltonian assuming the lattice dynamical problem has been solved.

The total pseudopotential is now given by

$$W(\underline{r}) = \sum_{\ell} w(\underline{r}-\underline{R}^{o}_{\ell}-\underline{u}_{\ell}) \tag{2.15}$$

with $\underline{u}_\ell$ the displacement from equilibrium of ion ℓ. $W(\underline{r})$ acts upon each electron separately. Expressed in the notation of second quantization it becomes

$$\sum_{\sigma} \int d^3r\ \psi^{\dagger}_{\sigma}(\underline{r})\langle\underline{r}|W|\underline{r}\rangle\psi_{\sigma}(\underline{r}) \tag{2.16}$$

where $\psi^{\dagger}_{\sigma}$ and ψ_σ are the usual field operators for an electron of spin σ at position $\underline{r}$. Expanding

$$\psi_\sigma(\underline{r}) = \sum_{\underline{k}} \langle\underline{r}|\phi_{\underline{k}}\rangle C_{\underline{k}\sigma},$$

with $C_{\underline{k}\sigma}$ the annihilation operator for an electron in state $|\phi_{\underline{k}}\rangle$, and performing the integral in (2.16) yields the expression

$$\sum_{\underline{k}\underline{k}'\sigma} \langle \phi_{\underline{k}'} | W | \phi_{\underline{k}} \rangle C^{\dagger}_{\underline{k}'\sigma} C_{\underline{k}\sigma} \tag{2.18}$$

for the pseudopotential operator.

Using (2.15) and (2.12) the matrix element is written as

$$\begin{aligned} \langle \phi_{\underline{k}'} | W | \phi_{\underline{k}} \rangle = {} & \frac{1}{\Omega} \sum_{nn'} a^{*}_{n'}(\underline{k}') a_n(\underline{k}) \\ & \times \sum_{\ell} \int d^3 r \, e^{-i(\underline{k}'+\underline{\kappa}_{n'})\cdot\underline{r}} w(\underline{r}-\underline{R}^{o}_{\ell}-\underline{u}_{\ell}) \\ & \times e^{i(\underline{k}+\underline{k}_n)\cdot\underline{r}} \, . \end{aligned} \tag{2.19}$$

Substituting $\underline{y} = \underline{r}-\underline{R}^{o}_{\ell}-\underline{u}_{\ell}$ into each term of the sum over ℓ gives for the integral in (2.19) the expression

$$e^{-i(\underline{k}'+\underline{\kappa}_{n'}-\underline{k}-\underline{\kappa}_n)\cdot(\underline{R}^{o}_{\ell}+\underline{u}_{\ell})} \; \frac{\Omega}{N} \langle \underline{k}'+\underline{\kappa}_{n'} | w | \underline{k}+\underline{\kappa}_n \rangle$$

where we normalize the plane waves to the volume per ion, $\frac{\Omega}{N}$, in the single-ion matrix element

$$\langle \underline{p}' | w | \underline{p} \rangle \equiv \frac{N}{\Omega} \int d^3 y \, e^{-i\underline{p}'\cdot\underline{y}} \, w(\underline{y}) e^{i\underline{p}\cdot\underline{y}} \, .$$

Assuming the ion displacements to be small, we expand the exponential to first order in the $\underline{u}_{\ell}$ and obtain for (2.19)

$$\begin{aligned} \langle \phi_{\underline{k}'} | W | \phi_{\underline{k}} \rangle = {} & \sum_{nn'} a^{*}_{n'}(\underline{k}) \langle \underline{k}'+\underline{\kappa}_{n'} | w | \underline{k}+\underline{}_n \rangle \\ & \times \frac{1}{N} \sum_{\ell} e^{-i(\underline{k}'+\underline{\kappa}'_{\underline{n}}-\underline{k}-\underline{\kappa}_n)\cdot R^{o}_{\ell}} \\ & \times \{1+i(\underline{k}'+\underline{\kappa}'_n-\underline{k}-\underline{\kappa}_n)\cdot\underline{u}_{\ell}\} \end{aligned} \tag{2.20}$$

The term which is independent of $\underline{u}_\ell$ describes the effect of the static lattice. Performing the sum over ℓ on this term provides a factor N and restricts $\underline{k}-\underline{k}'$ to a reciprocal lattice vector. Using this term together with the kinetic energy term gives a Schrödinger equation describing the band structure. Denoting the energy eigenvalues by $\varepsilon_{\underline{k}}$, we can write kinetic plus static-lattice contributions to the total Hamiltonian as $\sum_{\underline{k}\sigma} \varepsilon_{\underline{k}} C^\dagger_{\underline{k}\sigma} C_{\underline{k}\sigma}$.

To deal with the term involving the displacements $\underline{u}_\ell$, which are functions of time, we need to solve the lattice dynamics. We shall simply take the standard result derived, for example, in Maradudin (1969). In the harmonic approximation, the ion displacements are given by

$$\underline{u}_\ell = \left(\frac{\hbar}{2NM}\right)^{1/2} \sum_{q\lambda} \frac{\underline{\varepsilon}_\lambda(\underline{q})}{\sqrt{\omega_\lambda(\underline{q})}} e^{i\underline{q}\cdot R^0_\ell} \left(a^\dagger_{-q,\lambda}+a_{q,\lambda}\right) \qquad (2.21)$$

for a crystal containing N ions of mass M. $\underline{\varepsilon}_\lambda(\underline{q})$ and $\omega_\lambda(\underline{q})$ are respectively the normalized polarization vector and frequency of the crystal normal mode with polarization index λ and wavevector $\underline{q}$. The phonon operators $a^\dagger$ and a create and destroy an excitation (phonon) in the appropriate mode. We have the symmetry properties

$$\begin{aligned} \omega_\lambda(\underline{q}) &= \omega_\lambda(-\underline{q}) = \omega_\lambda(\underline{q}+\underline{\kappa}) \\ \varepsilon_\lambda(\underline{q}) &= \underline{\varepsilon}^*_\lambda(\underline{q}) = \underline{\varepsilon}_\lambda(\underline{q}+\underline{\kappa}) \end{aligned} \qquad (2.22)$$

for each reciprocal lattice vector $\underline{\kappa}$. In the Born-von Kármán theory, the frequencies and polarization vectors are derived from a small number of interionic force constants, which may be determined experimentally by fitting to inelastic neutron scattering data (Brockhouse et al, 1968).

Substituting (2.21) into (2.20) and performing the sum over ℓ gives a factor $N\delta_{\underline{q},\underline{k}'-\underline{k}}$, since $\underline{q}$ is unique only up to a reciprocal lattice vector. The sum over $\underline{q}$ from (2.21) may be performed trivially to give, for the phonon contribution to $<\phi_{\underline{k}'}|W|\phi_{\underline{k}}>$,

$$g_{\underline{k}',\underline{k};\lambda}(a^{\dagger}_{\underline{k}-\underline{k}',\lambda}+a_{\underline{k}'-\underline{k},\lambda}) \tag{2.23}$$

with

$$g_{\underline{k}',\underline{k};\lambda} = -i\sqrt{\frac{\hbar}{2MN\ \ (\underline{k}'-\underline{k})}}\ \underline{\varepsilon}_{\lambda}(\underline{k}'-\underline{k})$$

$$\cdot \sum_{nn'} a^{*}_{n'}(\underline{k}')a_{n}(\underline{k})\,(\underline{k}'+\underline{\kappa}_{n'},-\underline{k}-\underline{\kappa}_{n}) \tag{2.24}$$

$$\times <\underline{k}'+\underline{\kappa}_{n'}|w|\underline{k}+\underline{\kappa}_{n}>.$$

We have made use of the symmetry properties (2.22) to obtain this form. Finally, we substitute into (2.18) to obtain the electron-phonon contribution to the Hamiltonian

$$\mathcal{H}_{e-p} = \sum_{\substack{\underline{k}\underline{k}'\\ \sigma\lambda}} g_{\underline{k}',\underline{k};\lambda}\, c^{\dagger}_{\underline{k}'\sigma}c_{\underline{k}\sigma}(a^{\dagger}_{\underline{k}-\underline{k}',\lambda}+a_{\underline{k}'-\underline{k},\lambda}) \tag{2.25}$$

Note that $g_{\underline{k},\underline{k}';\lambda} = g^{*}_{\underline{k}',\underline{k};\lambda}$ so that $\mathcal{H}_{e-p}$ is Hermitian.

Given the phonon frequencies and polarization vectors, and the pseudopotential form factor $<\underline{p}'|w|\underline{p}>$, the electron-phonon coupling constant $g_{\underline{k}',\underline{k};\lambda}$ may be calculated approximately by truncating the expansion (2.12) of the pseudowavefunction after a few plane waves. For calculations to second order in the electron-phonon interaction, the required information on $g_{\underline{k}',\underline{k};\lambda}$ is contained more compactly in "effective weighted phonon frequency distributions" (Leung, 1974). We shall need only the function

$$\alpha^2_{\underline{k}}(\omega)F_{\underline{k}}(\omega) = \frac{\Omega}{(2\pi)^3\hbar^2}\sum_{\lambda}\int\frac{dS_{\underline{k}'}}{|v_{\underline{k}'}|}\,|g_{\underline{k},\underline{k}';\lambda}|^2\,\delta(\omega-\omega_{\lambda}(\underline{k}-\underline{k}')) \qquad (2.26)$$

which contains also the necessary information on the phonon frequencies and the Fermi surface. The integral is over the Fermi surface, with $S_{\underline{k}}$ a surface element. $v_{\underline{k}} \equiv \underline{\nabla}_{\underline{k}}\,\varepsilon_{\underline{k}}$ is the electron velocity.

Leavens and Carbotte (1971) calculated this function in Al using a single plane wave for the coupling constant and a spherical Fermi surface. Tomlinson and Carbotte (1976) used four plane waves for the coupling constant and for the Fermi surface. Leung (1974) described the Fermi surface with four plane waves, and used 15 plane waves for the electron-phonon interaction. All took phonon data from a Born-von Kármán fit to inelastic neutron scattering experiments.

We shall use the functions tabulated by Leung, which are the most realistic calculations available. For the Fermi surface he used the parameters of Ashcroft (1963) fitted to the de Haas-van Alphen data. The coupling constant was calcu-

Figure 1

The dimensionless function $\alpha_{\underline{p}}^{2}(\omega)F_{\underline{p}}(\omega)$, calculated by Leung (1974), at two points. The upper graph represents the point $\theta = 21°$, $\phi = 23°$ near a Bragg plane, and the lower graph is at the point $\theta = 53°$, $\phi = 45°$ in a free-electron-like region.

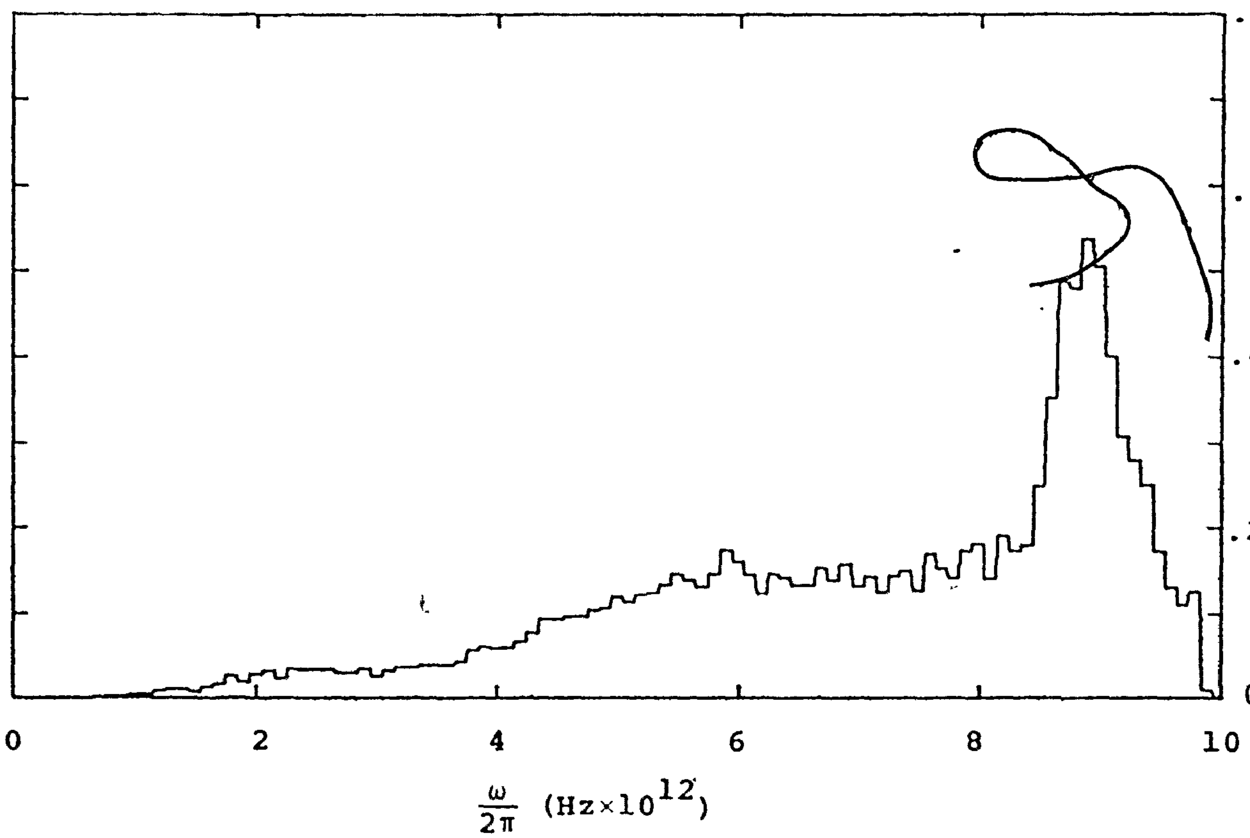
.8
.6
.4
.2
0
0
2
4
6
8
10
$\frac{\omega}{2\pi}$ (Hz×10^{12})

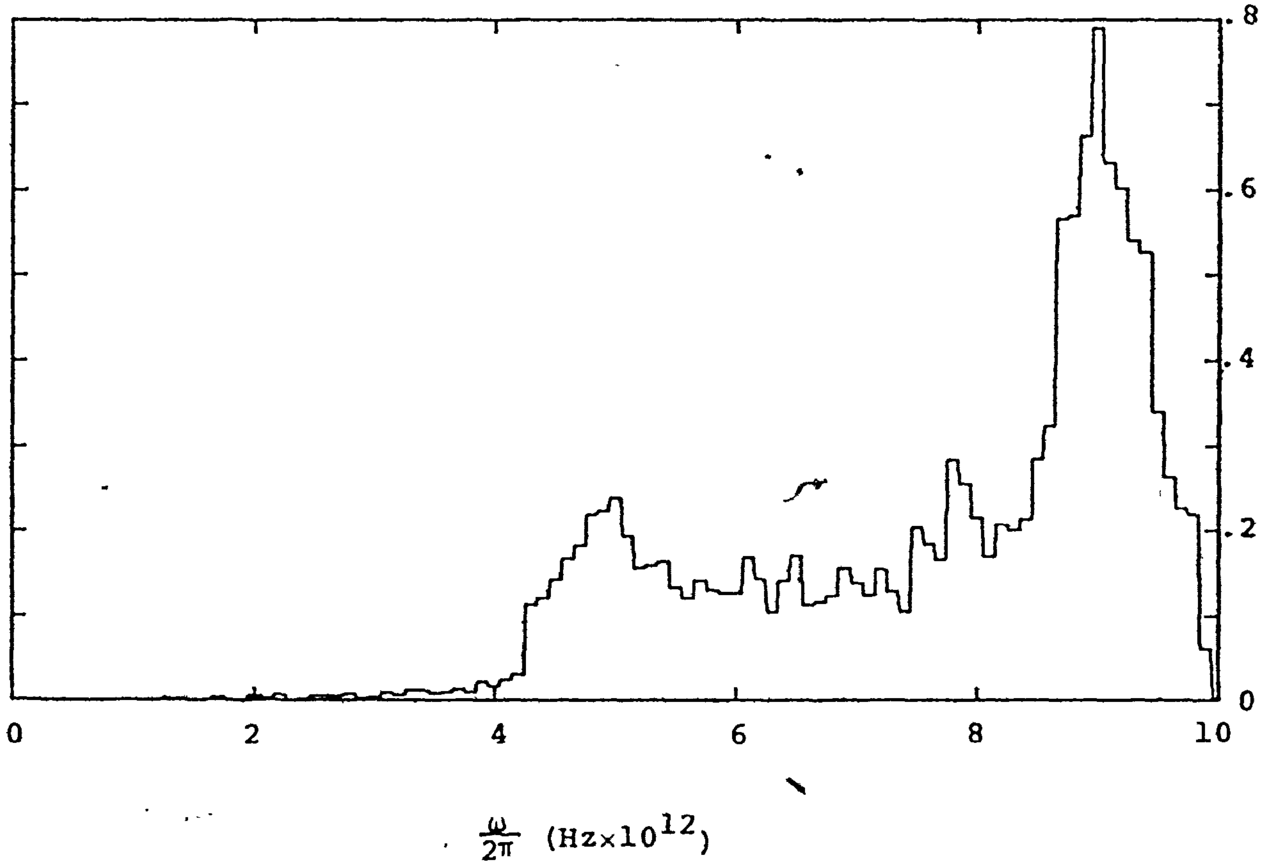
.8
.6
.4
.2
0
0
2
4
6
8
10
$\frac{\omega}{2\pi}$ (Hz×10^{12})

lated with the pseudopotential form factor computed by Animalu and Heine (1965) by the method of Heine and Abarenkov (1964). $\alpha^2_{\underline{k}}(\omega)F_{\underline{k}}(\omega)$ is given at 62 points $\underline{k}$ on the irreducible 1/48 of the Fermi surface as a histogram with 100 bins between zero and the maximum phonon frequency. Figure 1 shows Leung's $\alpha^2_{\underline{k}}(\omega)F_{\underline{k}}(\omega)$ as a function of frequency for two $\underline{k}$ points. The sharp peaks at high frequency, and the broader peaks at intermediate frequencies are characteristic of such distributions, and correspond to Van Hove singularities in the phonon density of states. Fluctuations from bin to bin which can be seen in figure 1 are an artifact of the method used to calculate the distributions in a reasonable amount of computer time, and are essentially statistical in origin.

CHAPTER III

QUASIPARTICLE PROPERTIES AT FINITE TEMPERATURE

3.1 Quasiparticles

The appearance of the phonon operators in H_{e-p} (2.25) modifies our picture of electrons in a metal. Instead of a Fermi sea of electrons in energy eigenstates moving through a self-consistent potential, we imagine electrons followed by lattice distortions, occasionally scattering off phonons to new momentum states. The fundamental electron-like excitation of the system, or quasiparticle, is an electron plus its attendant lattice distortion. It is described by a wavevector $\underline{k}$ and energy $E_{\underline{k}}$, in general differing from the band structure energy $\varepsilon_{\underline{k}}$. We define the self-energy Σ of the electron by

$$E_{\underline{k}} = \varepsilon_{\underline{k}} + \Sigma(E_{\underline{k}},\underline{k}) \ . \tag{3.1}$$

Since we shall use ordinary perturbation theory, Σ will correspond to the real part of the complex self-energy which arises in a Green's function approach (Scalapino, 1969). For convenience, we take $E_{\underline{k}}$ and $\varepsilon_{\underline{k}}$ to be measured from the Fermi energy μ, which is not shifted by the electron-phonon interaction.

In magnetic resonance experiments (for example, see Allen and Cohen, 1969) and other phenomena, the effect of the change in electron energy enters as an extra factor $(1 + \lambda_{\underline{k}})$ multiplying the appropriate band-structure effective mass. $\lambda_{\underline{k}}$, the electron mass renormalization parameter, is given by

$$\lambda_{\underline{k}} = - \left. \frac{d\Sigma(E_{\underline{k}},\underline{k})}{dE_{\underline{k}}} \right|_{E_{\underline{k}}=0} . \tag{3.2}$$

$E_{\underline{k}} = 0$ describes a state at the Fermi energy. Note that

$$E_{\underline{k}} \simeq \frac{\varepsilon_{\underline{k}}}{1 + \lambda_{\underline{k}}} \tag{3.3}$$

for small $\varepsilon_{\underline{k}}$.

Individual quasiparticle states are not eigenstates of the system Hamiltonian, but decay with a characteristic time $\tau_{\underline{k}}$, emitting or absorbing a phonon. The finite relaxation time ascribes a width to the quasiparticle energies according to the uncertainty principle. At zero temperature $\tau_{\underline{k}}$ is infinite for a state at the Fermi energy, but becomes rapidly shorter as temperature increases, limiting the range over which quasiparticle self-energies may be measured. $\tau_{\underline{k}}$ will be calculated in the final section of this chapter.

3.2 The Electron Mass Renormalization Parameter

We derive in this section an expression for $\lambda_{\underline{k}}(T)$ following the approach suggested by Wilkins (1968). Treating the electron-phonon interaction as a perturbation, we obtain the energy of the many-particle system at finite temperature, to second order in H_{e-p}. From this expression, the energy of a single quasiparticle is extracted, defining the electron mass renormalization parameter through (3.1) and (3.2). With some approximations, $\lambda_{\underline{k}}(T)$ is written as an integral over the function $\alpha^2_{\underline{k}}(\omega)F_{\underline{k}}(\omega)$ in a form facilitating numerical evaluation.

We take the system Hamiltonian to be

$$\begin{aligned} H &= \sum_{\underline{k}\sigma} \hat{n}_{\underline{k}} \, (\varepsilon_{\underline{k}}+\mu) + \sum_{\underline{q},\lambda}^{\mathrm{FBZ}} \hat{n}_{\underline{q}\lambda} \hbar\omega_\lambda(\underline{q}) + H_{e-p} \\ &\equiv H_0 + H_{e-p} \end{aligned} \tag{3.4}$$

with $\hat{n}_{\underline{k}\sigma} = c^\dagger_{\underline{k}\sigma}c_{\underline{k}\sigma}$ and $\hat{n}_{\underline{q}\lambda} = a^\dagger_{\underline{q},\lambda}a_{\underline{q}\lambda}$ the number operators for electrons and phonons. To second order in H_{e-p}, the energy E_g of a state $|g\rangle$ of the N-electron system is

$$E_g = E_g^{(0)} + \langle g|H_{e-p}|g\rangle + \sum_f \frac{|\langle g|H_{e-p}|f\rangle|^2}{E_g^{(0)}-E_f^{(0)}} \tag{3.5}$$

with

$$E_g^{(0)} = \langle g|H_0|g\rangle .$$

The sum is over a complete set of states $|f\rangle$. Since H_{e-p} contains one phonon operator per term in (2.25), the diagonal matrix element $\langle g|H_{e-p}|g\rangle$ vanishes. Using (2.25) we expand

$$\begin{aligned} |\langle g|H_{e-p}|f\rangle|^2 = \sum_{\substack{\underline{k}\underline{k}' \\ \sigma\lambda}} & |g_{\underline{k}',\underline{k};\lambda}|^2 \langle g|c^\dagger_{\underline{k}'\sigma}c_{\underline{k}\sigma}(a^\dagger_{\underline{k}-\underline{k}',\lambda}+a_{\underline{k}'-\underline{k},\lambda})|f\rangle \\ & \times \langle f|(a_{\underline{k}-\underline{k}'}, +a^\dagger_{\underline{k}'-\underline{k},\lambda})c^\dagger_{\underline{k}\sigma}c_{\underline{k}'\sigma}|g\rangle . \end{aligned} \tag{3.6}$$

Only the terms involving a phonon creation operator in one matrix element and a phonon annihilation operator in the other survive, giving

$$|\langle g|H_{e-p}|f\rangle|^2 = \sum_{\substack{\underline{k}\underline{k}'\\ \sigma\lambda}} |g_{\underline{k}',\underline{k};\lambda}|^2 \{\langle g|c^\dagger_{\underline{k}'\sigma}c_{\underline{k}\sigma}a^\dagger_{\underline{k}-\underline{k}',\lambda}|f\rangle \times \langle f|a_{\underline{k}-\underline{k}',\lambda}c^\dagger_{\underline{k}\sigma}c_{\underline{k}\sigma}|g\rangle + \langle g|c^\dagger_{\underline{k}'\sigma}c_{\underline{k}\sigma}a_{\underline{k}'-\underline{k},\lambda}|f\rangle\langle f|a^\dagger_{\underline{k}'-\underline{k},\lambda}c^\dagger_{\underline{k}\sigma}c_{\underline{k}'\sigma}|g\rangle \ . \tag{3.7}$$

The first term is zero unless the energy denominator in (3.5) is $\varepsilon_{\underline{k}'}-\varepsilon_{\underline{k}} + \hbar\omega_\lambda(\underline{k}-\underline{k}')$; similarly, for the second term, the energy denominator must be $\varepsilon_{\underline{k}'}-\varepsilon_{\underline{k}} - \hbar\omega_\lambda(\underline{k}'-\underline{k})$. Since we can avoid a reference to $E_f^{(0)}$ in the denominator we may perform the sum over f, treating $\sum_f |f\rangle\langle f|$ as a unit operator. With the aid of the commutation and anticommutation relations for boson and fermion operators, we obtain from (3.5)

$$E_g = \langle g|H_0|g\rangle + \sum_{\substack{\underline{k}\underline{k}'\\ \sigma\lambda}} |g_{\underline{k}',\underline{k};\lambda}|^2 \{\frac{\langle g|\hat{n}_{\underline{k}'\sigma}(1-\hat{n}_{\underline{k}\sigma})\hat{n}_{\underline{k}-\underline{k}',\lambda}|g\rangle}{\varepsilon_{\underline{k}'}-\varepsilon_{\underline{k}}+\hbar\omega_\lambda(\underline{k}-\underline{k}')} + \frac{\langle g|\hat{n}_{\underline{k}'\sigma}(1-\hat{n}_{\underline{k}\sigma})(1+\hat{n}_{\underline{k}'-\underline{k},\lambda})|g\rangle}{\varepsilon_{\underline{k}'}-\varepsilon_{\underline{k}}-\hbar\omega_\lambda(\underline{k}'-\underline{k})}\} \ . \tag{3.8}$$

It is now straightforward to calculate the energy of the system in equilibrium at temperature T by replacing matrix elements in the state $|g\rangle$ by averages in the grand canonical ensemble, defined as (Pathria, 1972)

$$\langle\hat{O}\rangle = \frac{\mathrm{Tr}\ \hat{O}\ e^{-\beta(H_0-\mu N)}}{\mathrm{Tr}\ e^{-\beta(H_0-\mu N)}}\ . \tag{3.9}$$

$\beta = 1/k_BT$, where k_B is Boltzmann's constant, the trace operation is denoted by Tr, and N is the total number operator for electrons; the chemical potential is zero for phonons.

The trace may be evaluated in a complete set of states characterized by their eigenvalues $n_{\underline{k}\sigma}$ and $\eta_{\underline{q}\lambda}$ of the electron and phonon number operators. Providing $\hat{O}$ is a function of the number operators, each term is simply a function of the occupation number eigenvalues. It is a standard trick to transform the sum over all possible sets of number eigenvalues to a product of sums over possible occupation numbers of each state. For example, for one of the terms in (3.8) we obtain

$$\langle\hat{n}_{k'\sigma}(1-\hat{n}_{\underline{k}\sigma})\hat{\eta}_{\underline{k}=\underline{k}'\lambda}\rangle = \frac{\sum\limits_n n e^{-\beta n\varepsilon_{\underline{k}'\sigma}}}{\sum\limits_n e^{-\beta n\varepsilon_{\underline{k}'\sigma}}} \times \frac{\sum\limits_n (1-n)e^{-\beta n\varepsilon_{\underline{k}\sigma}}}{\sum\limits_n e^{-\beta n\varepsilon_{\underline{k}\sigma}}} \times \frac{\sum\limits_{\eta=0}^{\infty} \eta e^{-\beta\eta\hbar\omega_\lambda(\underline{k}-\underline{k}')}}{\sum\limits_{\eta=0}^{\infty} e^{-\beta\eta\hbar\omega_\lambda(\underline{k}-\underline{k}')}} \tag{3.10}$$

since all other factors cancel out. The electron occupation number n may take the values 0 and 1, so those sums are trivially performed. The sums over the phonon occupation number η are, in the denominator, a geometric series, and in the numerator, the derivative of a geometric series, and may be evaluated analytically. It is apparent that each electron number operator $\hat{n}_{\underline{k}\sigma}$ in (3.8) gives rise to a factor

$$f(\varepsilon_{\underline{k}}) \equiv (e^{\beta\varepsilon_{\underline{k}}} + 1)^{-1} \tag{3.11}$$

and each phonon operator $\hat{n}_{\underline{q}\lambda}$ yields a factor

$$N(\omega_\lambda(q)) = (e^{\beta\hbar\omega_\lambda(\underline{q})} - 1)^{-1} . \tag{3.12}$$

For the energy $E_N(T)$ of the N-electron system in equilibrium at temperature T we finally obtain

$$\begin{aligned} E_N(T) = {} & \sum_{\underline{k}\sigma} (\varepsilon_{\underline{k}}+\mu) f(\varepsilon_{\underline{k}}) + \sum_{\underline{q}\lambda}^{FBZ} \hbar\omega_\lambda(\underline{q}) N(\omega_\lambda(\underline{q})) \\ & + \sum_{\substack{\underline{k}\underline{k}' \\ \sigma\lambda}} |g_{\underline{k}',\underline{k};\lambda}|^2 \{ \frac{f(\varepsilon_{\underline{k}'})(1-f(\varepsilon_{\underline{k}}))N(\omega_\lambda(\underline{k}-\underline{k}'))}{\varepsilon_{\underline{k}'}-\varepsilon_{\underline{k}}+\hbar\omega_\lambda(\underline{k}-\underline{k}')} \\ & + \frac{f(\varepsilon_{\underline{k}'})(1-f(\varepsilon_{\underline{k}}))1+N(\omega_\lambda(\underline{k}'-\underline{k}))}{\varepsilon_{\underline{k}'}-\varepsilon_{\underline{k}}-\hbar\omega_\lambda(\underline{k}'-\underline{k})} \}. \end{aligned} \tag{3.13}$$

To extract from this the energy due to a particular quasiparticle state, we consider the change in E_N due to a variation in the average occupation $\langle\hat{n}_{\underline{p}\sigma'}\rangle$ or $f(\varepsilon_{\underline{p}})$ of a state $\underline{p}\sigma'$, that is

$$
\begin{aligned}
E_{\underline{p}}(T) &= \frac{\delta E_N(T)}{\delta f(\varepsilon_{\underline{p}})} - \mu \\
&= \varepsilon_{\underline{p}} + \sum_{\underline{k}\lambda} |g_{\underline{p},\underline{k};\lambda}|^2 \Big\{ \frac{(1-f(\varepsilon_{\underline{k}}))N(\omega_\lambda(\underline{k}-\underline{p}))}{\varepsilon_{\underline{p}}-\varepsilon_{\underline{k}}+\hbar\omega_\lambda(k-p)} \\
&\quad + \frac{(1-f(\varepsilon_{\underline{k}}))[1+N(\omega_\lambda(\underline{p}-\underline{k}))]}{\varepsilon_{\underline{p}}-\varepsilon_{\underline{k}}-\hbar\omega_\lambda(\underline{p}-\underline{k})} \\
&\quad + \frac{f(\varepsilon_{\underline{k}})N(\omega_\lambda(\underline{p}-\underline{k}))}{\varepsilon_{\underline{p}}-\varepsilon_{\underline{k}}-\hbar\omega_\lambda(\underline{p}-\underline{k})} + \frac{f(\varepsilon_{\underline{k}})[1+N(\omega_\lambda(\underline{k}-\underline{p}))]}{\varepsilon_{\underline{p}}-\varepsilon_{\underline{k}}+\hbar\omega_\lambda(\underline{k}-\underline{p})} \Big\} ,
\end{aligned}
\tag{3.14}
$$

We have subtracted μ so as to measure $E_{\underline{p}}$ from the Fermi level, and have dropped the sum over σ since we are considering a state of particular spin when we take the derivative. In obtaining the form of the last two terms, we have used the symmetry of the coupling constant, $g_{\underline{k}',\underline{k};\lambda} = g^*_{\underline{k},\underline{k}';\lambda}$.

The expression (3.14) may be explained in a straightforward way. We can think of the electron-phonon interaction as inducing virtual scattering of an electron from one state to another and back, with the emission and absorption of a phonon (not necessarily in that order). Each scattering vertex gives a factor of the electron-phonon coupling constant, and we divide by the energy difference between the original and virtual states in the usual perturbation-theory fashion. If we put an electron in state $\underline{p}$, it scatters to all states $\underline{k}$, giving the first two terms in the sum over states in (3.14). The factor $1-f(\varepsilon_{\underline{k}})$ describes the Pauli-principle requirement that the state $\underline{k}$ be empty. The first term describes the absorption of a phonon by the electron in state $\underline{p}$, bringing in the phonon occupation factor. In the second term, the electron emits a phonon, giving rise to spontaneous emission and stimulated emission (the factor $N(\omega_\lambda)$) terms. By filling the state $\underline{p}$, we alter slightly the energy of the other states $\underline{k}$ by forbidding transitions to state $\underline{p}$. This contribution is described by the final two terms.

Treating (3.14) in this way as a perturbation-theory expression involving the single-particle states suggests the substitution $\varepsilon_{\underline{p}} \rightarrow E_{\underline{p}}$ in the energy denominators, equivalent to using Brillouin-Wigner perturbation theory in place of the Rayleigh-Schrödinger method. In this way we sum higher-order terms without extra work, and reproduce the Green's function result for the real part of the self-energy (Scalapino, 1969). Collecting terms with similar denominators in (3.14), and using the phonon symmetry $\omega_\lambda(\underline{q}) = \omega_\lambda(-\underline{q})$, we now write

$$\begin{aligned} \Sigma(E_{\underline{p}},\underline{p}) &= E_{\underline{p}} - \varepsilon_{\underline{p}} \\ &= \sum_{\underline{k}\lambda} |g_{\underline{p},\underline{k};\lambda}|^2 \Big\{\frac{f(\varepsilon_{\underline{k}})+N(\omega_\lambda(\underline{p}-\underline{k}))}{E_{\underline{p}}-\varepsilon_{\underline{k}}+\hbar\omega_\lambda(\underline{p}-\underline{k})} \\ &\quad + \frac{1-f(\varepsilon_{\underline{k}})+N(\omega_\lambda(\underline{p}-\underline{k}))}{E_{\underline{p}}-\varepsilon_{\underline{k}} - \hbar\omega_\lambda(\underline{p}-\underline{k})}\Big\} . \end{aligned} \tag{3.15}$$

We change the sum over $\underline{k}$ to an integral with the substitution

$$\sum_{\underline{k}} \rightarrow \frac{\Omega}{(2\pi)^3} \int \frac{dS_{\underline{k}} d\varepsilon_{\underline{k}}}{\hbar|v_{\underline{k}}|}$$

where $dS_{\underline{k}}$ is an area element in $\underline{k}$-space of a surface of constant $\varepsilon_{\underline{k}}$. $\varepsilon_{\underline{k}}$ is integrated from $-\mu$ to ∞ along paths perpendicular to the constant-energy surfaces, or parallel to $\underline{v}_{\underline{k}}$. We want the correction to the energy to be real, so the principal value of the integrals is assumed.

With a few remarks on the variation of the integrand in $\underline{k}$-space, we may separate the two integrations over area and energy for the states $\underline{p}$ of interest. We shall subsequently discover that the self-energy Σ is non-zero only for states within a phonon energy or so of the Fermi energy, so we restrict our attention to states $\underline{p}$ near the Fermi surface. The largest contribution to (3.15) comes from states $\underline{k}$ for which the energy denominators are small, that is, for $\varepsilon_{\underline{k}}$ within a phonon energy of $E_{\underline{p}}$. Because we have restricted $\underline{p}$ to the region near the Fermi surface, this implies that only states $\underline{k}$ within a phonon energy or two of the Fermi energy will contribute significantly to Σ. As we integrate over $\varepsilon_{\underline{k}}$, along a direction perpendicular to the constant-energy surfaces, we may therefore disregard contributions from the regions where $\underline{k}$ differs from the Fermi wavevector by more than about $\omega/v_{\underline{k}} \times k_f$ (in magnitude) or $\frac{\hbar\omega}{2(\varepsilon_{\underline{k}}+\mu)} k_f$ for a free-electron system. For aluminum, we are therefore interested in $|\underline{k}|$ within about .25% of its Fermi-surface value. Obviously, we may perform the integral over $\varepsilon_{\underline{k}}$ regarding as constant such factors as $|v_{\underline{k}}|$ which vary with $\underline{k}$ scale of the magnitude $|k|$.

The coupling constant $g_{\underline{p},\underline{k};\lambda}$ and the phonon frequency $\omega_\lambda(\underline{p}-\underline{k})$ both vary on the scale of $|\underline{p}-\underline{k}|$ as we change $\underline{k}$. However, we may disregard the regions where $\underline{p}-\underline{k}$ is small compared to $|k|$. In the long-wavelength limit, $\omega(\underline{q}) \propto \underline{q}$ and the pseudopotential form factor goes to a constant non-zero value. By (2.24), $|g_{\underline{p},\underline{k};\lambda}|^2 \propto |\underline{p}-\underline{k}|$ as $\underline{k}\to\underline{p}$, cancelling the $1/\omega$ divergence of $N(\omega)$. The number of states contributing to (3.15) for a particular value of $|\underline{p}-\underline{k}|$ and $\varepsilon_{\underline{k}}$ is proportional to $|\underline{p}-\underline{k}|$ at small momentum transfer, and so we may treat $\underline{p}-\underline{k}$ as being sufficiently large that it does not vary much as $\varepsilon_{\underline{k}}$ varies between about $\pm\, h\omega$.

We have finally arrived at the point where we may perform the integration over energy treating $\omega_\lambda(\underline{p}-\underline{k})$, $g_{\underline{p},\underline{k};\lambda}$ and $v_{\underline{k}}$ as constant. The phonon factors now vanish since they may be taken outside the energy integral, and

$$\int_{-\infty}^{\infty} dx\left[\frac{1}{x+y} + \frac{1}{x-y}\right] = 0$$

where, of course, we are taking principal values, and the range of integration may be extended from $-\mu$ to $-\infty$ for the energies $E_{\underline{p}}$ of interest.

We are left with, from (3.15)

$$\Sigma(E_{\underline{p}},\underline{p}) = \frac{\Omega}{(2\pi)^3}\int \frac{dS_{\underline{k}}}{\hbar|v_{\underline{k}}|}\,|g_{\underline{p},\underline{k};\lambda}|^2 \times \int_{-\infty}^{\infty} d\varepsilon\left\{\frac{f(\varepsilon)}{E_{\underline{p}}-\varepsilon+\hbar\omega_\lambda} + \frac{1-f(\varepsilon)}{E_{\underline{p}}-\varepsilon-\hbar\omega_\lambda(\underline{p}-\underline{k}}\right\}. \qquad (3.16)$$

Making a change of variables $\varepsilon \to -E_{\underline{p}}+\varepsilon$ in the first term and $\varepsilon \to E_p-\varepsilon$ in the second, and using the relation $f(x) = 1-f(-x)$ gives for the energy integral

$$\int_{-\infty}^{\infty} d\varepsilon \, \frac{f(\varepsilon-E_{\underline{p}}) - f(\varepsilon+E_{\underline{p}})}{\varepsilon - \hbar\omega_\lambda(\underline{p}-\underline{k})} \quad .$$

At $E_{\underline{p}} = 0$ the integrand vanishes, so $\Sigma(0,\underline{p}) = 0$. With (3.1), this implies that the Fermi energy is not shifted by the electron-phonon interaction. The numerator $f(\varepsilon-E_{\underline{p}})-f(\varepsilon+E_{\underline{p}})$ is non-zero and constant for ε between $\pm E_{\underline{p}}$ and zero elsewhere, with a rounding of the corners to a distance $\sim k_B T$. As $E_{\underline{p}}$ increases above a few times the maximum phonon frequency, the integral, and thus the self-energy, falls off like $1/E_{\underline{p}}$. We can therefore evaluate the surface integral in (3.16) over the Fermi surface for all $E_{\underline{p}}$ of interest, rather than over the surface $\varepsilon_{\underline{k}} = E_{\underline{p}}$. Introducing the factor

$$\int_0^{\infty} d\omega \delta(\omega-\omega_\lambda(\underline{p}-\underline{k})) = 1$$

into (3.16) and using the definition (2.26), we obtain

$$\Sigma(E,\underline{p}) = \hbar \int_0^{\infty} d\omega \, \alpha^2_{\underline{p}}(\omega) F_{\underline{p}}(\omega) \int_{-\infty}^{\infty} d\varepsilon \, \frac{f(\varepsilon-E) - f(\varepsilon+E)}{\varepsilon - \hbar\omega} \quad . \qquad (3.17)$$

In this expression the self-energy depends separately on the energy E (measured from the Fermi level) of a quasiparticle and on the position $\underline{p}$ on the Fermi surface closest to the actual quasiparticle wavevector. By restricting $\underline{p}$ to the Fermi surface, we have introduced a fractional error of the order of a phonon energy divided by the Fermi energy, $\sim$ 1% at most.

Using (3.2) and (3.17) we obtain an expression for the mass renormalization parameter,

$$\lambda_{\underline{p}}(T) = 2\hbar \int_0^\infty d\omega\ \alpha^2_{\underline{p}}(\omega)F_{\underline{p}}(\omega) \int_{-\infty}^{\infty} d\varepsilon\ \frac{f'(\varepsilon)}{\varepsilon-\hbar\omega} \qquad (3.18)$$

where $f'(\varepsilon) = \frac{df(\varepsilon)}{d\varepsilon}$. Even in taking derivatives we are justified in treating E and $\underline{p}$ as independent variables. Σ varies with $\underline{p}$ on the scale of a Fermi wavevector, and with E on the scale of phonon and thermal energies. $\nabla_{\underline{p}} E_{\underline{p}}$ is a (renormalized) Fermi velocity, so the term $\frac{\partial\Sigma}{\partial p}\frac{d\underline{p}}{dE}$ which we have ignored is of the order of the ratio of the sound velocity to the Fermi velocity, again ∿ 1%, times the term $\frac{\partial\Sigma}{\partial E}$ which has been retained.

The behaviour of (3.18) will be discussed more fully in the next chapter when we outline the calculations, but we shall point out here that at T=0 the function f'(ε) becomes the Dirac delta δ(ε), so we obtain at zero temperature

$$\lambda_{\underline{p}}(0) = 2 \int_0^\infty \frac{d\omega}{\omega}\ \alpha^2_{\underline{p}}(\omega)F_{\underline{p}}(\omega). \qquad (3.19)$$

This is the familiar expression appearing in the work of Leavens and Carbotte (1971) and of Leung (1974) on the anisotropy of the electron-phonon interaction in aluminum.

3.3 The Quasiparticle Lifetime

A quasiparticle near the Fermi energy does not remain in the same state indefinitely, but scatters via the electron-phonon interaction to states nearby in energy, with the emission or absorption of a phonon. The decay rate is described in a Green's function approach (Fetter and Walecka, 1971) by the imaginary part of a complex self-energy, obtained by subtracting $i\delta$ from $E_{\underline{p}}$ in (3.16), where δ is a positive infinitesimal. We shall use an approach based on the Fermi golden rule, after Wilkins (1968).

Again we begin with an N-electron system in state $|g\rangle$. By the golden rule, the decay rate from this state is given by

$$\Gamma_g = \frac{2\pi}{\hbar} \sum_f |\langle g|H_{e-p}|f\rangle|^2 \delta(E_g - E_f). \tag{3.20}$$

Since we are interested in a system at (or near) equilibrium at temperature T, we again average over states $|g\rangle$ in the grand canonical ensemble. We can proceed exactly as we did in evaluating the self-energy, replacing energy denominators with energy δ-functions. We obtain an expression analogous to the expression (3.13) for the total system energy. This averaged decay rate, which we label Γ_{eq}, refers to the equilibrium distribution over states in the ensemble, and must be zero. Invoking the detailed balance condition, we may require more specifically that the ensemble-averaged occupancy of each particle state be constant in time. If we now alter slightly the occupancy of state $\underline{p}$, the decay of the system to new states is entirely due to scattering to and from state $\underline{p}$, and we may identify the relaxation rate $\frac{1}{\tau_{\underline{p}}}$ with the functional derivative $\delta\Gamma_{eq}/\delta f(\varepsilon_{\underline{p}})$. Compare this with (3.14), where the quasiparticle energy was equated with the derivative $\delta E_N/\delta f(\varepsilon_{\underline{p}}) - \mu$. Without trudging through the same mathematics twice, we write from inspection of (3.15),

$$\frac{1}{\tau_{\underline{p}}} = \frac{2\pi}{\hbar} \sum_{\underline{k}\lambda} |g_{\underline{p},\underline{k};\lambda}|^2 \{[f(\varepsilon_{\underline{k}})+N(\omega_\lambda(\underline{p}-\underline{k}))] \times \delta(E_{\underline{p}}-\varepsilon_{\underline{k}}+\hbar\omega_\lambda(\underline{p}-\underline{k})) + [1-f(\varepsilon_{\underline{k}})+N(\omega_\lambda(\underline{p}-\underline{k})]\delta(E_{\underline{p}}-\varepsilon_{\underline{k}}-\hbar\omega_\lambda(\underline{p}-\underline{k}))\}. \tag{3.21}$$

We take $\underline{p}$ to be near the Fermi surface, and change the sum to an integral

$$\sum_{\underline{k}} \rightarrow \frac{\Omega}{(2\pi)^3} \int_{FS} \frac{dS_{\underline{k}}}{\hbar|v_{\underline{k}}|} \int_{-\infty}^{\infty} d\varepsilon_{\underline{k}}$$

where the δ-functions in (3.21) restrict $\underline{k}$ to the region of the Fermi surface and by arguments similar to those used in deriving (3.16) we may perform the two integrations independently. Again we introduce the factor

$$\int_0^\infty \delta(\omega-\omega_\lambda(\underline{p}-\underline{k}))d\omega = 1$$

and after performing the energy integral, obtain

$$\frac{1}{\tau_{\underline{p}}(E,T)} = 2\pi \int_0^\infty d\omega\ \alpha^2_{\underline{p}}(\omega)F_{\underline{p}}(\omega)\{2N(\omega)+f(\hbar\omega+E)+f(\hbar\omega-E)\}. \qquad (3.22)$$

It is of interest to estimate the behaviour of the relaxation time at low temperature and energy. $N(\omega)$ falls off exponentially for $\hbar\omega$ above about $2k_BT$, as the Fermi functions do for $\hbar\omega$ greater than $|E| + k_BT$. Only the low-frequency part of $\alpha^2_{\underline{p}}(\omega)F_{\underline{p}}(\omega)$ will be significant in the region of low E and T. Since the phonon frequencies $\omega_\lambda(\underline{q})$ are zero for $\underline{q}$ equal to a reciprocal lattice vector, the low frequency contributions in (2.26) arise from those portions of the Fermi surface integral where $\underline{k}-\underline{k}'$ is close to some $\underline{\kappa}$. The frequencies $\omega_\lambda(\underline{q})$ are evenly distributed in $\underline{q}$-space and proportional to $|q|$ at low frequency. Within a mode λ, the frequency will be constant as $\underline{k}'$ moves about $\underline{k}$ in a closed curve whose perimeter will be proportional to ω_λ if the phonon anisotropy does not change rapidly as frequency increases. As was argued earlier, $|g_{\underline{k},\underline{k}';\lambda}|^2$ is also proportional to $\omega_\lambda(\underline{k}-\underline{k}')$ in the low-frequency regions. We should expect $\alpha^2_p(\omega)F_p(\omega)$ to vary as ω^2 at 'sufficiently' low frequencies, although it is hard to estimate quantitatively what range this will encompass in polyvalent metals, which have Umklapp processes across the Fermi surface at zero phonon frequency for certain points $\underline{k}$.

Taking (3.22) at T=0 and E small but positive, and defining the step function $\theta(x)$ as equal to 1 for positive x and zero for negative x, we have

$$\frac{1}{\tau(E,0)} \propto \int_0^\infty d\omega\ \omega^2\ \theta(E-\hbar\omega)$$

which implies, since $\tau(E,0) = \tau(-E,0)$,

$$\frac{1}{\tau(E,0)} \propto |E|^3 \tag{3.23}$$

for small $|E|$.

If we set E=0 in (3.22) the weight function in curly brackets becomes a function of $\hbar\omega/k_BT$ only, so for T small,

$$\frac{1}{\tau(0,T)} \propto \int_0^\infty \omega^2\ g\left(\frac{\hbar\omega}{k_BT}\right)d\omega$$

since the exponential decrease of g at large argument allows us to ignore the contributions to the integral in the regions where ω^2 is a bad approximation to the true distribution. Setting $\frac{\hbar\omega}{k_BT} \to x$ gives a definite integral in x whose value is independent of T, with a factor $(k_BT/\hbar)^3$ in front. So at low temperatures,

$$\frac{1}{\tau(0,T)} \propto T^3 . \tag{3.24}$$

It is worth noting that experiments cannot be performed at T=0 or in general at E=0. We shall simply state that the dominant effect of allowing E and T to be simultaneously non-zero is to add a constant to the right hand side of relations (3.23) and (3.24). The proof involves making an appropriate change of variables for each function in (3.22) and examining the resulting terms in the regions $E >> k_B T$ and $k_B T >> E$.

CHAPTER IV

CALCULATIONS AND RESULTS

4.1 The Aluminum Fermi Surface

We discuss in this chapter the formulae developed in Chapter III for λ and τ and the methods used to evaluate them numerically. The results are presented at a few temperatures and energies as a function of position on the Fermi surface. We list the values at 62 points in $\underline{k}$-space of a few parameters describing $\lambda_{\underline{k}}(T)$ and $\tau_{\underline{k}}(E,T)$ in regions accessible to experiment. Where such exist, experimental values and previous calculations are compared with the present results.

We begin by presenting a map (Fig. 2) of the irreducible 1/48th of the Fermi surface as calculated by Leung (1974) from Ashcroft's (1963) parameters. $\theta=0$ is a cube edge, $\theta=45°$, $\phi=0$ a face diagonal, and $\theta=54.7°$, $\phi=45°$ a body diagonal. (Aluminum has a face-centred cubic structure.) In certain directions the Fermi surface does not exist, with empty and filled states being separated by a Bragg plane in these regions. On our map (Fig. 2) the Fermi surface is divided in this way into four sections. Sections I and IV form a hole surface in the second band when reduced back to

Figure 2

Irreducible 1/47'th of the Al Fermi surface. In the shaded regions the Fermi surface does not exist. θ=0° is a cube edge, θ=45°, φ=0° is a face diagonal, and θ = 54.7°, φ = 45° is a body diagonal.

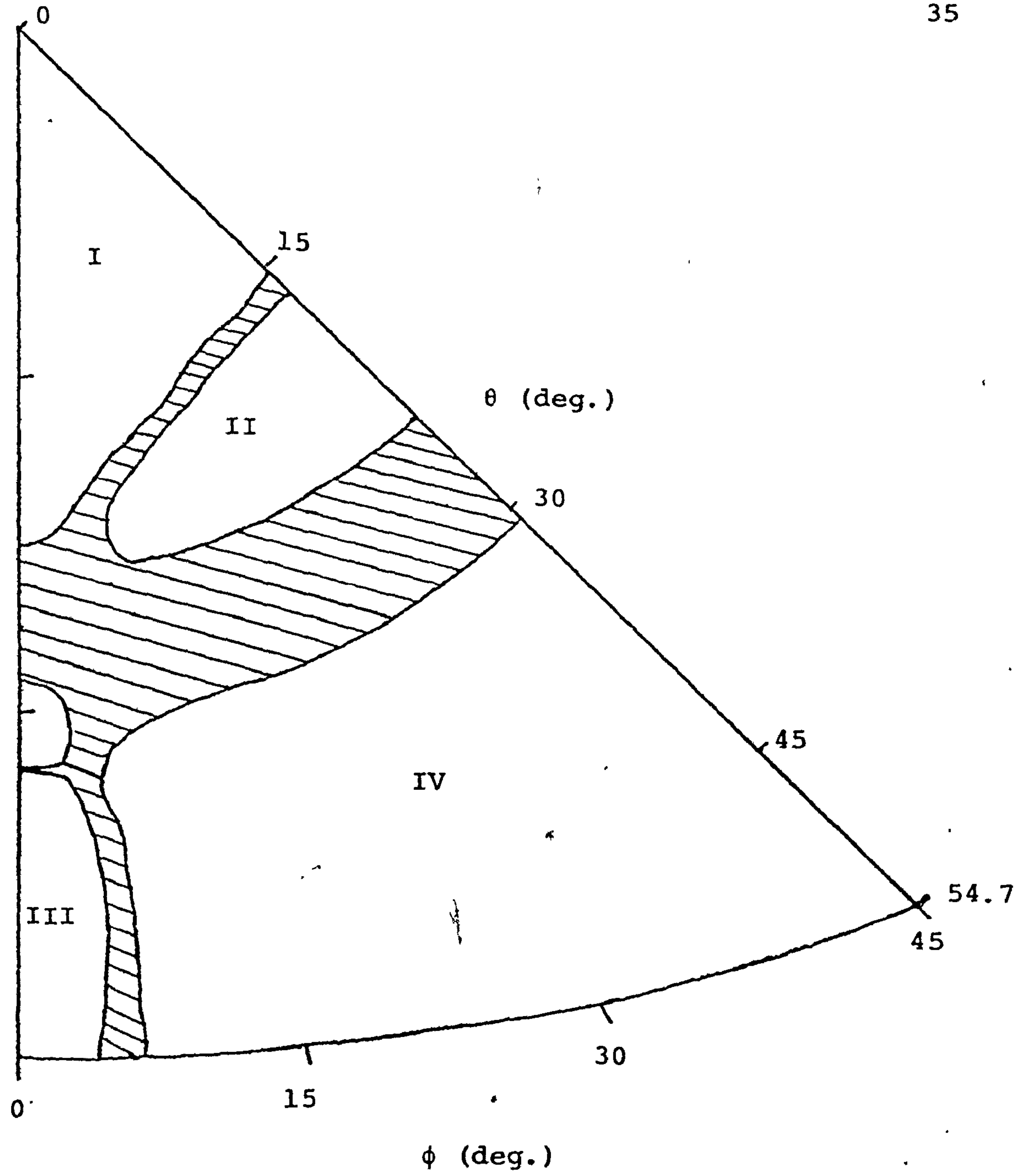
0
15
30
45
54.7
θ (deg.)
I
II
III
IV
0
15
30
45
φ (deg.)

the first Brillouin zone. The remaining pieces comprise an electron-surface 'monster' in the third band. We refer to Harrison (1966) for a fuller discussion of the Fermi-surface shape.

Section I and the upper edge of section II intersect the $(\frac{1}{2}\ \frac{1}{2}\ \frac{1}{2})$ plane. Between the points W and U which lie in directions $\theta=26.6°$, $\phi=0°$ and $\theta=19.5°$, $\phi=45°$ respectively, the planes $(\frac{1}{2}\ \frac{1}{2}\ \frac{1}{2})$ and (001) intersect. The lower edge of section II and the upper edges of sections III and IV end at the (001) plane. Along the boundary of the 1/48'th from W to the point K in the direction $\theta=45°$, $\phi=0°$ the $(\frac{1}{2}\ \frac{1}{2}\ \frac{1}{2})$ plane intersects the $(\frac{1}{2}\ -\frac{1}{2}\ \frac{1}{2})$ plane. The left-hand edge of surface IV and the right-hand edge of surface III are bounded by this $(\frac{1}{2}\ -\frac{1}{2}\ \frac{1}{2})$ plane. At about $\theta=32°$, section III is divided into two parts as the upper piece bends inward to cut the $(\frac{1}{2}\ -\frac{1}{2}\ \frac{1}{2})$ plane, and the lower piece curves outward to the (001) plane. The 62 points at which Leung's distributions are calculated are distributed over all 4 sections with a concentration near the Bragg planes, where the electronic properties may be expected to vary rapidly.

With these remarks as an aid to orienting the reader in momentum space, we proceed to a description of the calculations.

4.2 The Computations

For the purpose of numerical calculation, the formula (3-18) for $\lambda(T)$ may be written in the more convenient form

$$\lambda_{\underline{p}}(T) = 2\int_0^\infty \frac{d\omega}{\omega}\,\alpha_{\underline{p}}^2(\omega)F_{\underline{p}}(\omega)\{1 - \int_{-\infty}^\infty \frac{xe^x dx}{(1+e^x)^2) x-\beta\hbar\omega)}\} \ . \qquad (4.1)$$

We have substituted $\beta\varepsilon \rightarrow x$ and written

$$\frac{1}{x-\beta\hbar\omega} \equiv \frac{1}{\beta\hbar\omega}\left(\frac{x}{x-\beta\hbar\omega} - 1\right)$$

in order to extract a factor $\frac{1}{\omega}$ from the energy integral. It will simplify the logic of the computer programs to deal with the dimensionless quantities $\frac{d\omega}{\omega}$ and $\beta\hbar\omega$.

To evaluate the integral

$$\int_{-\infty}^\infty \frac{xe^x dx}{(1+e^x)^2(x-\beta\hbar\omega)} \qquad (4.2)$$

as a function of $\beta\hbar\omega$, we must consider the behaviour of the integrand. We are only interested in the principal value but the singularity at $x = \beta\hbar\omega$ has an unhealthy effect on convergence of numerical algorithms. It may be removed by integrating the sum of the contributions from either side of $x = \beta\hbar\omega$ over half the range of the integral (4.2). More explicitly, we substitute $x - \beta\hbar\omega \rightarrow y$ for $x > \beta\hbar\omega$ and $x - \beta\hbar\omega \rightarrow -y$ for $x < \beta\hbar\omega$, to obtain

$$\int_{-\infty}^{\infty} \frac{xe^{x}dx}{(1+e^{x})^{2}(x-\beta\hbar\omega)} = \int_{0}^{\infty} \frac{dye^{\beta\hbar\omega}}{y} \{\frac{(\beta\hbar\omega+y)e^{y}}{(1+e^{\beta\hbar\omega+y})^{2}} - \frac{(\beta\hbar\omega+y)e^{y}}{(1+e^{\beta h\omega-y})^{2}}\} . \qquad (4.3)$$

Because of the cancellation of terms at y=0, the integrand on the right hand side is finite everywhere, which facilitates the numerical integration. An accuracy of 3 digits in λ was deemed sufficient in view of the limitations of the available distributions $\alpha^{2}(\omega)F(\omega)$ (and of possible experiments) which requires that the integral (4-3) be calculated to an accuracy of 10^{-3}. In practice it was calculated to a precision of 10^{-5}, requiring less than a doubling of computer time for the integration subroutine and avoiding some problems of spurious convergence of the algorithm for small values of $\beta\hbar\omega$. The range of integration was truncated at a value above which the contribution of the exponential tail could be assumed to be negligible, and the resulting definite integral was evaluated on the McMaster CDC 6400 computer using Simpson's rule. Convergence to within 10^{-5} was obtained after 5 or 6 iterations (a total of 33 or 65 points at which the integrand was evaluated). A hundred evaluations of the integral (4.3), sufficient to calculate λ at one value of temperature from (4.1), required about a second of computer time. Because of the histogram nature of the tabulated functions $\alpha_{\underline{k}}^{2}(\omega)F_{\underline{k}}(\omega)$, a simple discrete sum was used for the frequency integration, with ω

Figure 3 a)

Calculated $\lambda_{\underline{k}}(T)/\lambda_{\underline{k}}(0)$ plotted against temperature for 4 points (θ,ϕ) as follows:

——— (1°,1°)

.... (21°,1°)

- - - - (17°,35°)

-·-·-·- (23°,45°)

Figure 3 b)

Calculated $\lambda_{\underline{k}}(T)/\lambda_{\underline{k}}(0)$ vs. temperature for 4 points (θ,ϕ):

——— (45°,1°)

.... (41°,50°)

- - - - (53°,45°)

-·-·-·- (31°,45°)

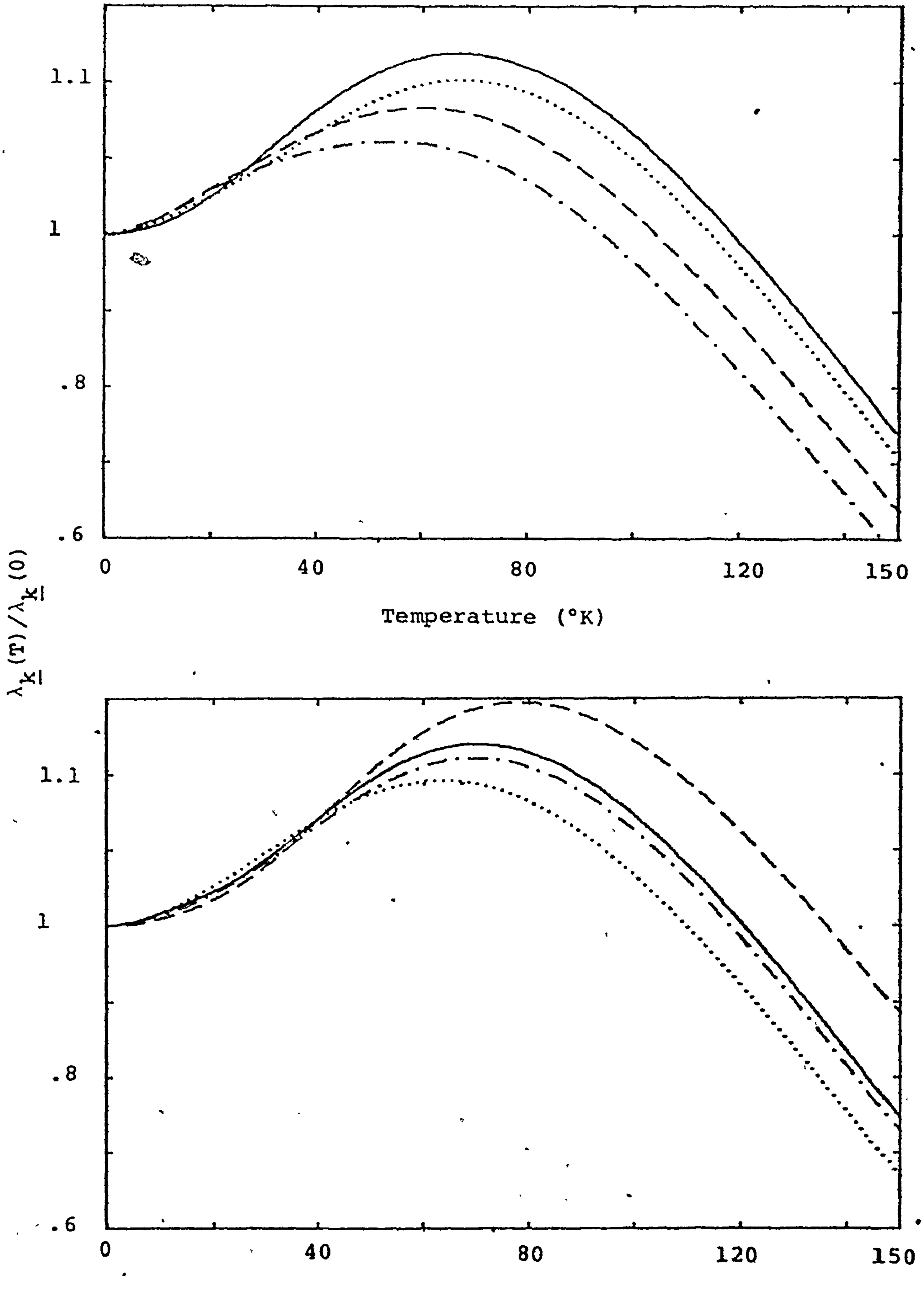
1.1
1
.8
.6
0
40
80
120
150
Temperature (°K)
$\lambda_{\underline{k}}(T)/\lambda_{\underline{k}}(0)$
1.1
1
.8
.6
0
40
80
120
150

values taken to be at the centres of the histogram bins.

Evaluating expression (3.22) for the relaxation time was much simpler, as only a single integration, over frequency ω, is involved. Again the frequency integration was performed simply by summing over the 100 values of ω at which the distributions are given. However, since the statistical factors in (3.22) can vary rapidly with ω at low temperatures, it was necessary to average them over the width of each histogram bin (rather than simply taking the value at the centre of the bin) in order to obtain τ as a reasonably smooth function of E and T.

4.3 Results

In Fig. 3a) and b) we display $\lambda_{\underline{k}}$ as a function of temperature, normalized to unity at T=0, for 8 points $\underline{k}$ on the Fermi surface. The overall shape of the curves is a general feature of such calculations, and was first discussed by Grimvall (1968) in an Einstein model. Starting From T=0, $\lambda_{\underline{k}}$ rises to a maximum at about 65°K in our aluminum calculations, then falls off gradually, going to zero like T^{-2} at high temperatures. It is apparent from fig. 3, however, that quantitative differences in behaviour exist between different states $\underline{k}$ on the Fermi surface. This anisotropy in $\lambda_{\underline{k}}(T)$ is displayed in another way in fig. 4a), b) and c), in which $\lambda_{\underline{k}}(T)$ at three temperatures is plotted as a function of angle θ along three constant-ϕ arcs.

Table I lists a few numbers which characterise the temperature-dependent mass enhancement at each of the 62 points on the irreducible 1/48'th. In addition to the values of $\lambda_{\underline{k}}$

Figure 4

$\lambda_{\underline{k}}(T)$ plotted along constant-ϕ arcs on the Fermi surface.

The temperatures are:

——— 0°K
.... 30°K
- - - - 50°K

Figure 4 a) (lower graph) is along the arc $\phi = 1°$.

4 b) is along the arc $\phi = 23°$

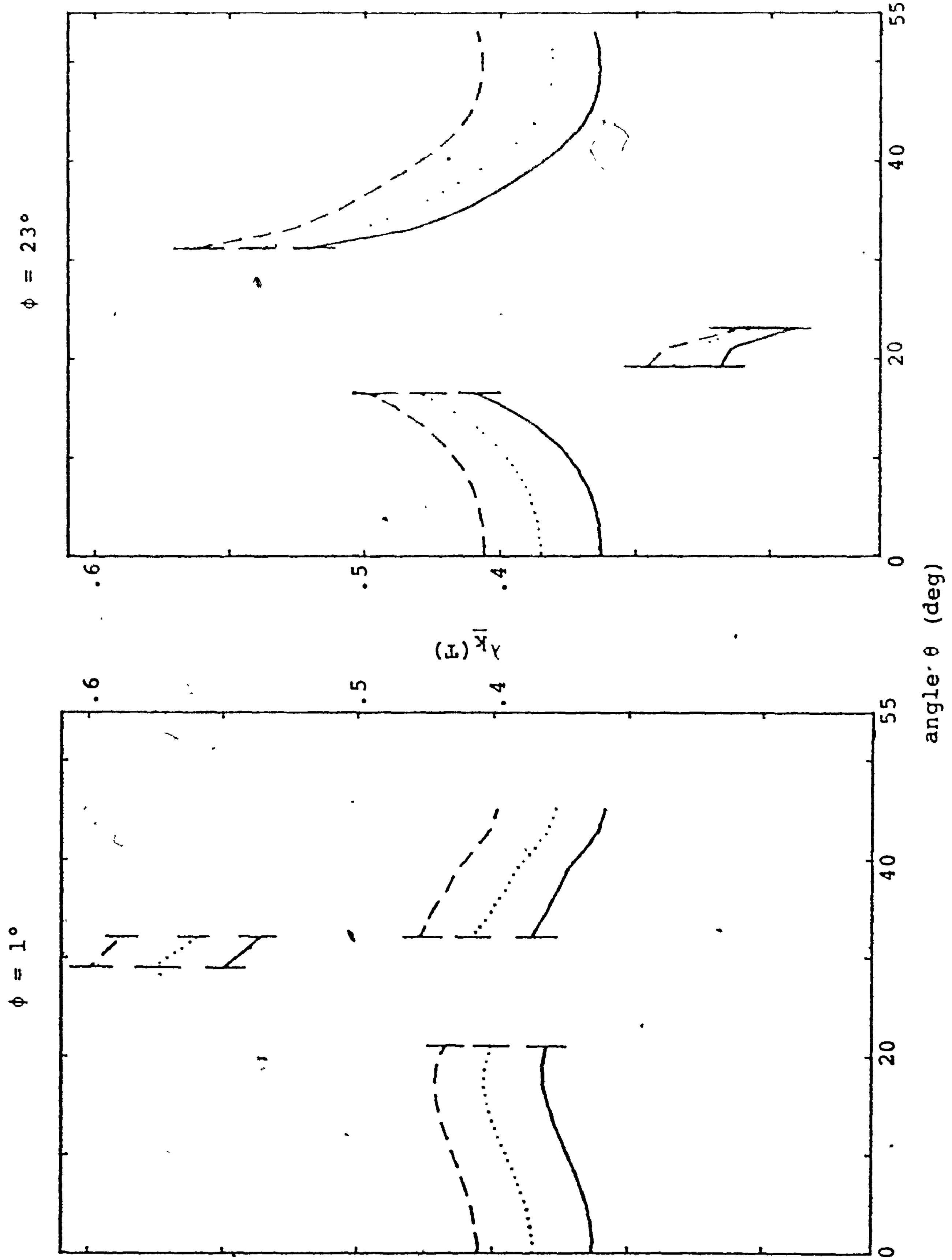
φ = 1°
φ = 23°
.6
.5
.4
$\lambda_{\bar{K}}(T)$
0
20
40
55
angle θ (deg)

Figure 4 c)

$\lambda_{\underline{k}}(T)$ along the Fermi-surface arc $\phi=45°$. The temperatures are:

——— 0°K

.... 30°K

- - - - 50°K

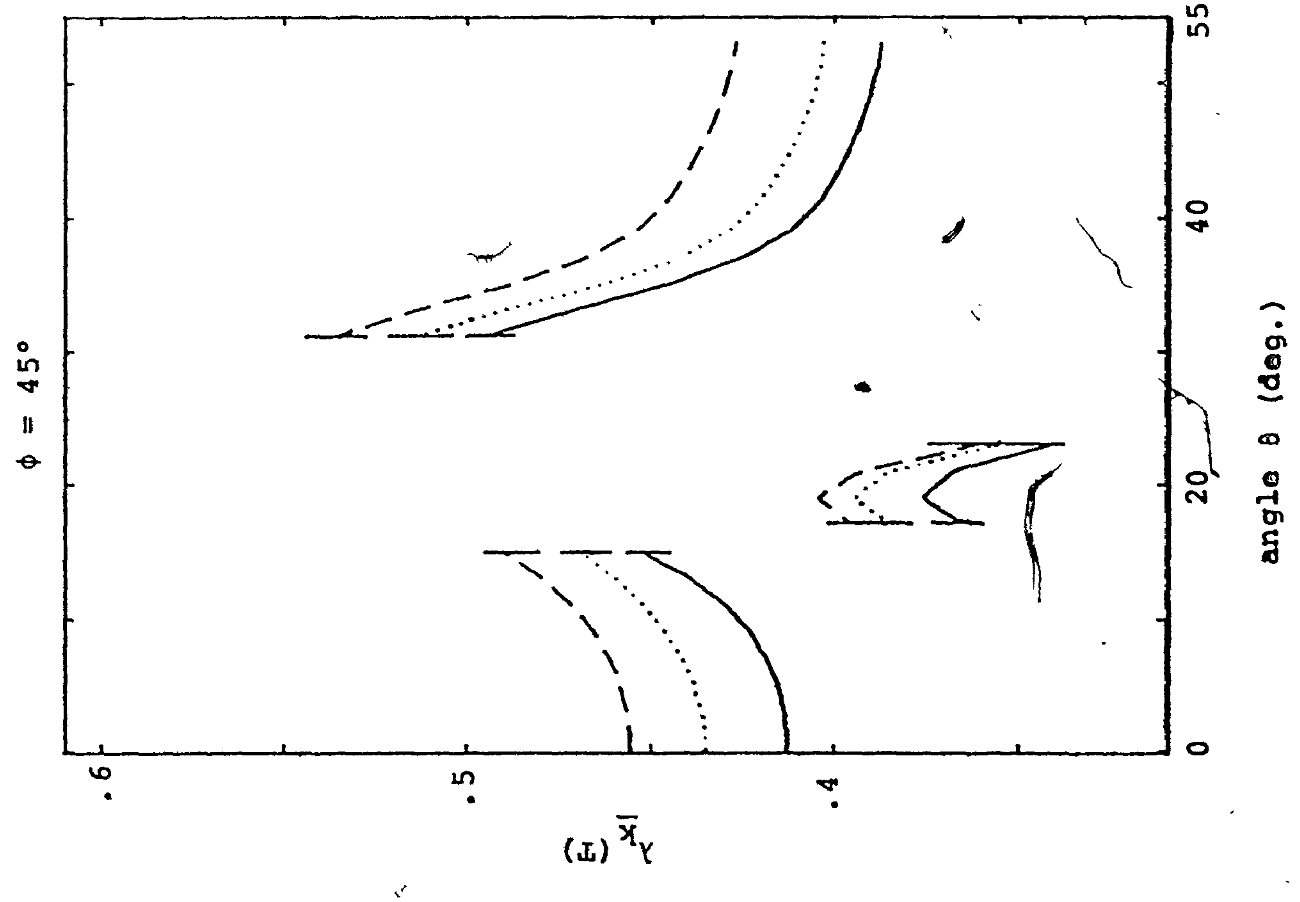
φ = 45°
$\lambda_{\bar{K}}$ (T)
.6
.5
.4
0
20
40
55
angle θ (deg.)

Table 1

Temperature dependence of $\lambda_{\underline{k}}(T)$

T_m is the temperature at which $\lambda_{\underline{k}}$ reaches a maximum

No.	(θ,ϕ) in deg.	$\lambda_{\underline{k}}(0)$	$\lambda_{\underline{k}}(30°)/\lambda_{\underline{k}}(0)$	T_m (°K)	$\lambda_{\underline{k}}(T_m)/\lambda_{\underline{k}}(0)$
SURFACE I					
1	(1, 1)	.413	1.054	67	1.119
2	(9, 1)	.421	1.054	66	1.115
3	(21, 1)	.430	1.046	67	1.102
4	(9, 9)	.421	1.054	66	1.115
5	(17, 9)	.442	1.043	67	1.105
6	(9,23)	.422	1.054	66	1.115
7	(15,23)	.448	1.045	68	1.106
8	(9,35)	.423	1.054	66	1.114
9	(13,35)	.445	1.050	67	1.108
10	(9,45)	.423	1.054	66	1.114
11	(13,45)	.440	1.046	70	1.110
SURFACE II					
12	(23, 9)	.350	1.042	62	1.072
13	(21,11)	.366	1.044	61	1.075
14	(19,17)	.362	1.048	60	1.080
15	(21,15)	.363	1.045	60	1.072
16	(23,15)	.353	1.044	59	1.065
17	(19,23)	.369	1.047	60	1.077
18	(21,23)	.365	1.045	59	1.070
19	(23,23)	.341	1.046	56	1.063
20	(17,35)	.364	1.051	59	1.034
21	(21,35)	.371	1.045	59	1.070
22	(23,35)	.344	1.049	55	1.065
23	(17,45)	.355	1.052	59	1.094
24	(21,45)	.368	1.047	58	1.071
25	(23,45)	.341	1.046	53	1.052
SURFACE III					
26	(29, 1)	.549	1.049	67	1.106
27	(31, 1)	.541	1.046	68	1.113
28	(33, 1)	.467	1.048	69	1.117
29	(37, 1)	.426	1.045	70	1.117
30	(41, 1)	.415	1.044	70	1.120
31	(45, 1)	.409	1.044	70	1.120
32	(31, 3)	.539	1.046	68	1.113
33	(35, 3)	.413	1.045	68	1.110
34	(37, 3)	.407	1.046	69	1.114
35	(41, 3)	.407	1.045	70	1.119
36	(41, 5)	.357	1.049	63	1.096
37	(43, 5)	.365	1.049	65	1.105
38	(45, 3)	.375	1.047	68	1.111

(continued next page)

Table 1 (continued)

No.	(θ,ϕ) in deg.)	$\lambda_{\underline{k}}(0)$	$\frac{\lambda_{\underline{k}}(30°)}{\lambda_{\underline{k}}(0)}$	T_m (°K)	$\frac{\lambda_{\underline{k}}(T_m)}{\lambda_{\underline{k}}(0)}$
SURFACE IV					
39	(31, 7)	.541	1.045	69	1.112
40	(33, 7)	.512	1.044	70	1.119
41	(35, 9)	.496	1.045	72	1.128
42	(45, 9)	.467	1.044	74	1.135
43	(31,15)	.523	1.042	70	1.111
44	(33,15)	.494	1.045	71	1.123
45	(35,15)	.473	1.046	72	1.132
46	(43,15)	.440	1.045	74	1.142
47	(47,15)	.437	1.045	75	1.143
48	(31,23)	.522	1.042	70	1.109
49	(35,23)	.463	1.045	74	1.134
50	(43,23)	.421	1.043	76	1.145
51	(49,23)	.413	1.042	76	1.147
52	(31,35)	.501	1.041	71	1.106
53	(33,35)	.469	1.042	73	1.122
54	(35,35)	.448	1.043	74	1.133
55	(43,35)	.404	1.041	77	1.147
56	(51,35)	.393	1.040	78	1.148
57	(31,45)	.496	1.041	71	1.105
58	(33,45)	.471	1.043	73	1.122
59	(35,45)	.444	1.043	75	1.133
60	(43,45)	.400	1.041	77	1.146
61	(53,45)	.387	1.040	78	1.147
62	(33,23)	.482	1.044	72	1.124

at zero temperature, calculated by Leung (1974), we list the temperature at which $\lambda_{\underline{k}}$ reaches its maximum, and the ratio of this maximum value to that at T=0. We give the ratio $\lambda_{\underline{k}}(T)/\lambda_{\underline{k}}(0)$ at 30° as well, as this is typically the maximum temperature at which experiments measuring quasiparticle properties in aluminum are currently performed (Doezema and Koch, 1975).

From Table I, the maximum increase of $\lambda_{\underline{k}}$ over its zero-temperature value varies between 6% and 15%, the peaks occurring at temperatures which correlate fairly well with the peak height, between 53°K for the lowest maxima and 78°K for the free-electron-like regions where the maximum increase of $\lambda_{\underline{k}}$ is largest. For comparison, the Einstein model considered by Grimvall (1968) would give a maximum in $\lambda(T)/\lambda(0)$ of 1.21 at a temperature of 0.28 times the Einstein temperature θ_E.

On the sections of the Fermi surface labelled I, II and III in figure 2, $\lambda_{\underline{k}}\max/\lambda_{\underline{k}}(0)$ is small, less than 1.12, and does not vary strongly over a given section. All the higher values are found around the points (53,45) on section IV. There is a smooth trend to higher values as one moves away from the Bragg planes everywhere except on section II, where $\lambda_{\underline{k}}\max/\lambda_{\underline{k}}(0)$ tends to increase as θ increases from the intersection with the $(\frac{1}{2}\,\frac{1}{2}\,\frac{1}{2})$ plane down to the (001) plane, which cuts the Fermi surface at about $\theta = 24°$.

Most of the variation in the temperature dependence of $\lambda_{\underline{k}}$ may be attributed to the anisotropy in the electron wavefunctions. Longitudinal phonons contribute more strongly to the electron-phonon coupling, as the factor $\underset{\sim}{\varepsilon}_\lambda \cdot (\underline{k}' + \underline{\kappa}_{n'} - \underline{k} - \underline{\kappa}_n)$ is small for normal processes if $\underset{\sim}{\varepsilon}_\lambda$ refers to a transverse phonon and n=n'. To the extent that the resulting strong peak in α^2F at high frequencies contains the major contribution to the effective frequency distribution, $\lambda_{\underline{k}}(T)$ approaches the Einstein-model value, with a maximum increase of 21% over its zero-temperature value. Even for a free-electron model, of course, there will be umklapp processes which contribute to a transverse-phonon peak at intermediate frequencies. As we approach a Bragg plane, however, there is a considerable mixing of states with $\underline{\kappa}_n \neq 0$, which can lead to umklapp processes at low frequency. Because of the higher density of states at low frequency for transverse phonons, the resulting increase in the coupling to low-frequency phonons can be considerable (compare the two distributions in figure 1, the upper one representing a point near the (001) plane, the lower one coming from a free-electron-like region). We note that the anisotropy in $\lambda_{\underline{k}}(0)$ follows a much different pattern; Leavens and Carbotte (1971) found that much of the variation in the zero-temperature value arises from the anisotropy of the phonons.

In figures 5, 6 and 7 we plot the lifetime τ against angle θ along 3 constant-ϕ arcs. The left-hand plots, labelled a), show $\tau(E,T=0)$ for energies of 1, 2 and 5 meV and the right-hand plots display $\tau(E=0,T)$ for 5°, 10° and 20°K.

Figure 5

The calculated $\tau_{\underline{k}}(E,T)$ plotted along the Fermi surface arc $\phi = 1°$.

5 b): E = 0, 3 temperatures:

———— 5°K

.... 10°K

- - - - 20°K

5a): T = 0, 3 energies:

———— 1 meV

.... 2 meV

- - - - 5 meV

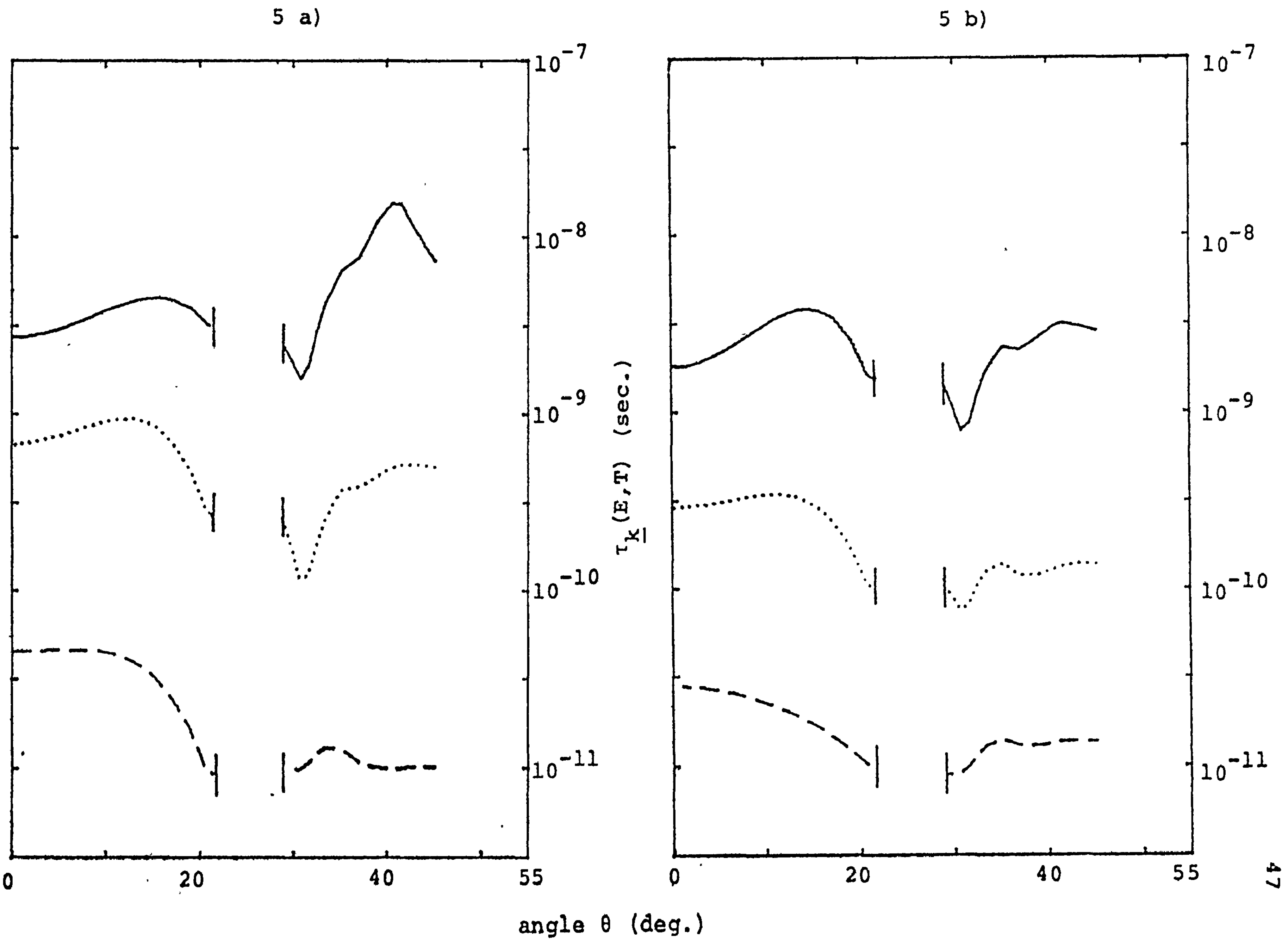
5 a)
5 b)
10^{-7}
10^{-8}
10^{-9}
10^{-10}
10^{-11}
$\tau_{\underline{k}}(E,T)$ (sec.)
0
20
40
55
angle θ (deg.)

Figure 6

The calculated $\tau_{\underline{k}}(E,T)$ plotted along the Fermi surface arc $\phi = 23°$.

6 b) E = 0, 3 temperatures:

——— 5°K

.... 10°K

- - - - 20°K

6 a) T = 0, 3 energies:

——— 1 meV

.... 2 meV

- - - - 5 meV

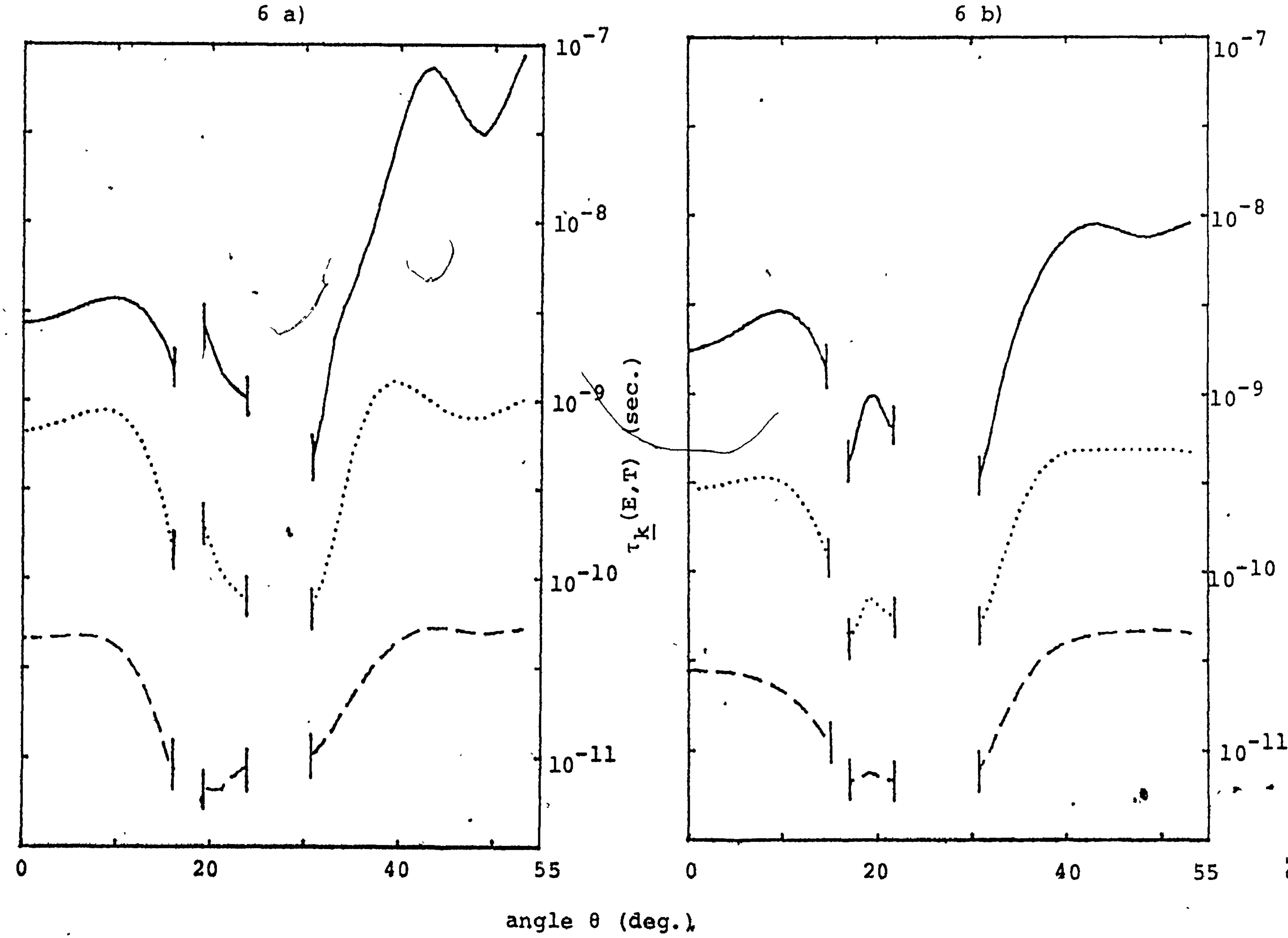
6 a)
6 b)
10^{-7}
10^{-8}
10^{-9}
10^{-10}
10^{-11}
$\tau_{\underline{k}}(E,T)$ (sec.)
0
20
40
55
angle θ (deg.)

Figure 7

The calculated $\tau_{\underline{k}}(E,T)$ plotted along the Fermi surface arc $\phi = 45°$.

7 b) E = 0, 3 temperatures:

——— 5°K

.... 10°K

- - - - 20°K

7a) T = 0, 3 energies:

——— 1 meV

.... 2 meV

- - - - 5 meV

7 a)

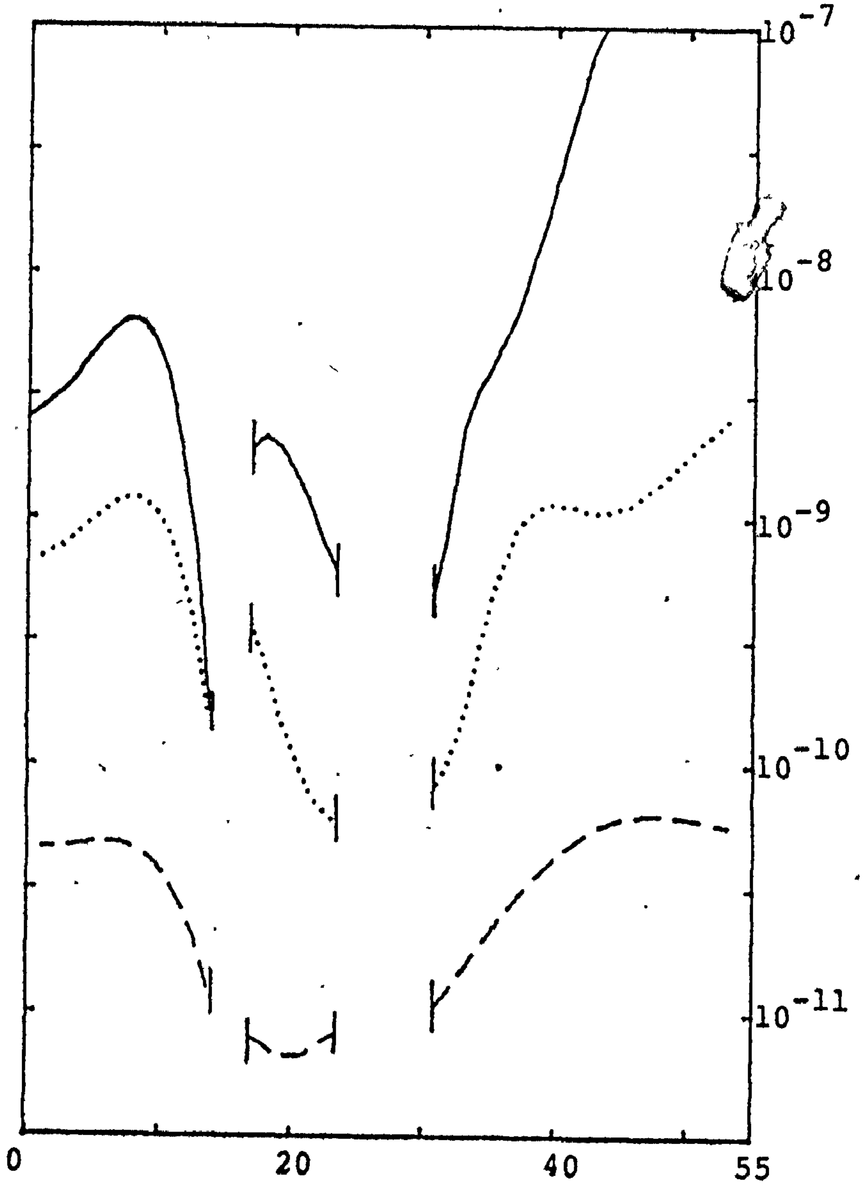
10^-7
10^-8
10^-9
10^-10
10^-11
0
20
40
55

7 b)

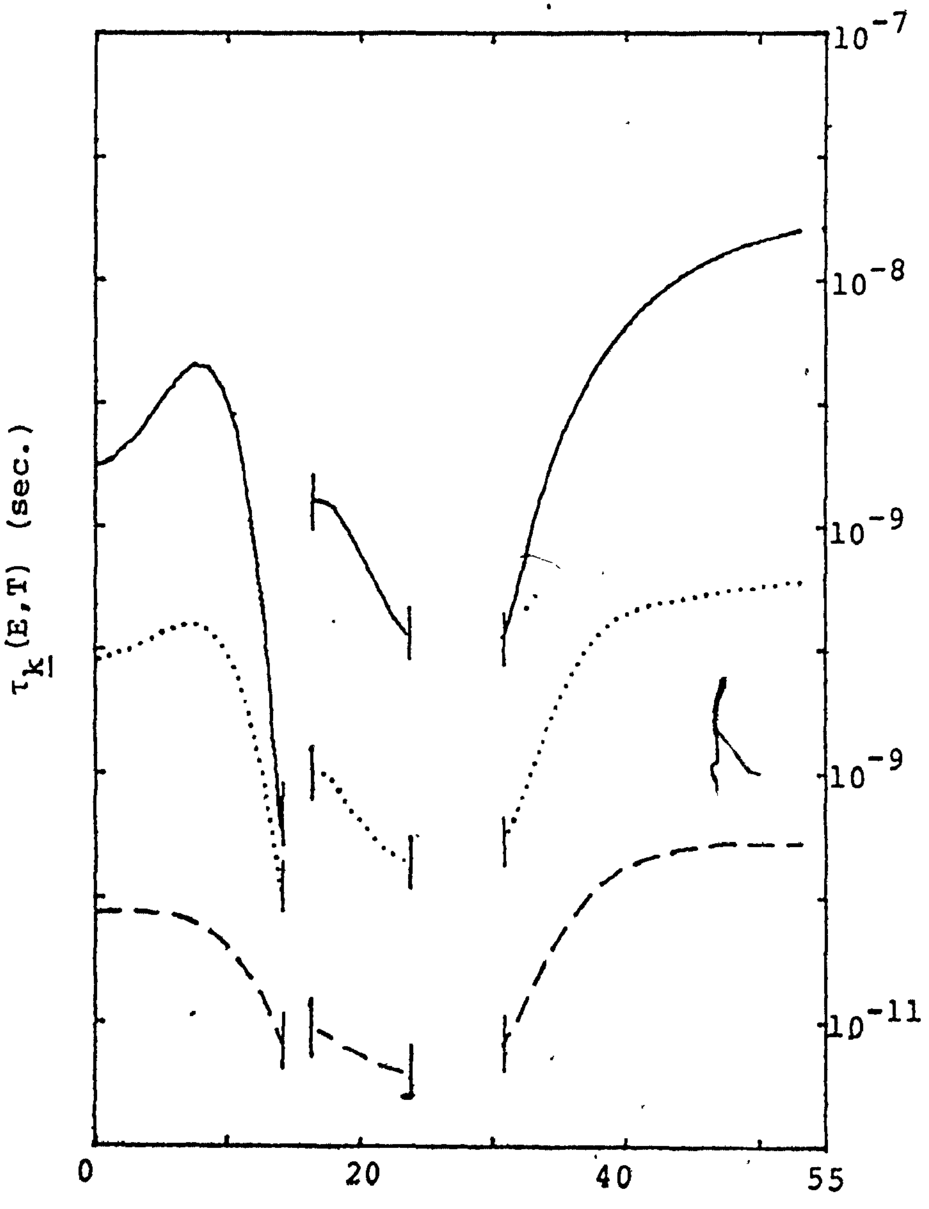
10^-7
10^-8
10^-9
10^-9
10^-11
0
20
40
55
τ_k(E,T) (sec.)
angle θ)deg.),

Note that τ is plotted on a logarithmic scale; the variation with position on the Fermi surface is very large. In general, lifetimes are lowest near Bragg planes, in keeping with our discussion of the anisotropy of λ, since the inverse of the lifetime is proportional to the low-frequency part of α^2F.

Much of the anisotropy tends to disappear at higher temperatures and energies, but not uniformly as we would expect if $1/\tau$ were proportional to T^3 and E^3 on the entire Fermi surface. Accordingly, the inverse lifetimes obtained were fitted to a general power law over the range 5-10°K for E=0 and 1-3 meV for T=0. The exponents α_E and α_T of the best fit are listed in table 2, along with the slopes of the best E^3 and ^{3} fits in the same range, and the values of α_T obtained by Tomlinson and Carbotte (1976) at 15 points. Our exponents are in general not particularly close to 3, nor do they always agree well with the results of Tomlinson's essentially similar calculation. Along the $\phi=45°$ arc, Tomlinson's use of only 4 plane waves might account for some differences, particularly near the high-symmetry direction (54.7°, 45°). Tomlinson's Fermi surface calculation differed from Leung's only in detail, but on narrow electron arm along $\phi=1°$, this may have improved his results.

Doezema and Wegehaupt (1975) have measured quasiparticle lifetimes in aluminum by observations of transitions between surface Landau levels. The technique involves measuring the surface impedance at microwave frequencies of a

Table 2

Parameters of the best fits $\tau^{-1}(E,0) \propto E^{\alpha_E}$, $\tau^{-1}(0,) \propto T^{\alpha_T}$, and $\tau^{-1}(E,0) = AE^3$, $\tau^{-1}(0,T) = BT^3$, over the range 1-3 meV, 5-10°K. The values of Tomlinson & Carbotte (1976) were fitted from 5-9°K.

No.	(θ,ϕ) in deg.	A 10^9 s^{-1}/ meV^3	α_E	B 10^6 s^{-1}/ $°K^3$	α_T	α_T (Tomlinson)
SURFACE I						
1	(1, 1)	.223	2.67	3.56	2.64	3.14
2	(9, 1)	.193	2.69	2.68	3.09	3.07
3	(21, 1)	.669	3.37	9.32	3.95	3.30
4	(9, 9)	.182	2.70	2.87	3.11	
5	(17, 9)	.406	3.40	6.80	3.68	
6	(9,23)	.182	2.72	2.88	3.13	
7	(15,23)	.585	3.23	8.47	3.44	
8	(9,35)	.179	2.82	2.31	3.21	
9	(13,35)	.286	3.09	4.71	3.49	
10	(9,45)	.171	3.22	2.50	3.57	3.47
11	(13,45)	.436	1.84	14.0	1.78	2.97
SURFACE II						
12	(23, 9)	1.35	3.70	15.8	3.59	
13	(21,11)	1.26	3.67	16.2	3.59	
14	(19,17)	.915	3.39	13.0	3.62	
15	(21,15)	1.28	3.75	16.0	3.66	
16	(23,15)	1.14	2.99	16.8	3.33	
17	(19,23)	.902	3.97	12.4	4.05	
18	(21,23)	1.25	3.40	16.7	3.56	
19	(23,23)	1.38	3.20	17.6	3.29	
20	(17,35)	.532	2.95	9.24	3.51	
21	(21,35)	1.30	3.35	17.6	3.49	
22	(23,35)	1.41	3.08	18.4	3.20	
23	(17,45)	.439	3.25	8.04	3.76	4.37
24	(21,45)	1.33	3.25	17.9	3.42	
25	(23,45)	1.77	2.84	23.5	3.04	3.09
SURFACE III						
26	(29, 1)	.563	3.19	8.84	3.77	2.37
27	(31, 1)	1.08	3.03	14.3	3.25	3.11
28	(33, 1)	.554	3.45	7.78	3.66	
29	(37, 1)	.554	4.53	7.66	4.22	4.29
30	(41, 1)	.472	5.05	6.62	4.54	
31	(45, 1)	.389	4.03	6.40	4.36	3.18
32	(31, 3)	.961	3.42	12.4	3.51	
33	(35, 3)	.700	3.03	9.94	3.44	
34	(37, 3)	.621	3.74	8.24	3.71	
35	(41, 3)	.689	3.80	8.34	3.65	
36	(41, 5)	.763	2.20	12.4	2.82	
37	(43, 5)	.678	2.35	10.4	2.83	
38	(45, 3)	.593	3.97	7.53	3.76	

(continued next page)

Table 2 (continued)

No.	(θ,ϕ) in deg.	A $\frac{10^9\ s^{-1}}{meV^3}$	α_E	B $\frac{10^6\ s^{-1}}{°K^3}$	α_T	α_T (Tomlinson)
SURFACE IV						
39	(31, 7)	1.11	3.10	14.9	3.35	
40	(33, 7)	.830	3.31	11.0	3.79	
41	(35, 9)	.309	3.45	5.28	4.11	
42	(45, 9)	.264	5.23	3.56	4.45	
43	(31,15)	1.57	2.40	22.5	2.71	
44	(33,15)	.778	3.28	9.98	3.23	
45	(35,15)	.276	2.98	4.60	3.59	
46	(43,15)	.153	5.24	1.99	4.24	
47	(47,15)	.142	4.52	1.92	3.99	
48	(31,23)	1.48	2.45	21.6	2.73	
49	(35,23)	.247	2.85	4.23	3.51	
50	(43,23)	.151	5.32	1.88	4.18	
51	(49,23)	.146	4.47	1.90	3.91	
52	(31,35)	1.53	2.58	20.9	2.85	
53	(33,35)	.815	3.39	10.2	3.33	
54	(35,35)	.249	3.11	4.10	3.73	
55	(43,35)	.149	5.43	1.85	4.20	
56	(51,35)	.126	7.18	1.45	4.68	
57	(31,45)	1.41	2.54	20.7	2.75	2.83
58	(33,45)	.722	3.30	9.26	3.34	
59	(35,45)	.279	2.89	4.61	3.48	4.00
60	(43,45)	.149	5.47	1.83	4.19	4.35
61	(53,45)	.131	7.70	1.46	4.65	3.23
62	(33,23)	.721	3.40	9.19	3.37	

sample with a magnetic field aligned parallel to the surface. Transitions are induced between states of an electron pinned to the surface by the $e\underline{v}\times\underline{B}$ force. From the position and width of peaks in the magnetic field derivative of the surface resistance (the experiments are performed at constant microwave frequency) and a detailed knowledge of the band structure, the electron mass renormalization parameter and the lifetime can be inferred. Unlike other magnetic-resonance techniques, which involve averaging around an orbit, the surface-Landau level experiments give point values, or at least averages over a small rectangle on the Fermi surface. Doezema and Koch (1975) give a fuller discussion of the method.

Table 3 gives the results of Doezema and Wegehaupt for $\tau^{-1}(E=0,T)/T^3$, as well as our and Tomlinson's calculated values. Their experiments were performed between 2° and 20°K, and they report that the T^3 law was obeyed at all 3 points, whereas we found exponents of 2.6, 1.8 and 4.7 (from table 2). The agreement with experiment in table 3 is good at (1°,1°), a factor of 2 at (13,45), and a factor of 2.5 at (53,45). The second point was close to the Bragg plane, where the lifetime varies rapidly; the factor of 2 does not necessarily represent a severe disagreement. At (53,45), however, we are in the centre of a large free-electron-like region, and the discrepancy is significant. The low value of the calculated $1/\tau$ and its rapid ($T^{4.7}$) increase with temperature may indicate that a reduced weighting of the first few frequency bins as an artifact of the calculation is at fault.

Table 3

A comparison of our coefficients $B = \langle \tau^{-1}(0,T)/T^3 \rangle$ with the experimental results of Doezema and Wegehaupt (1975) and with the values they inferred from Tomlinson's results at 5°K.

(θ,ϕ) in deg.	B (expt.)	B (our calc) ($10^6\ s^{-1}/°K^3$)	B(Tomlinson)
(1,1)	4.1±.3	3.6	3.4
(13,45)	31 ± 3	14	21
(53,45)	3.9±.3	1.5	1.4

CHAPTER V

CONCLUSION

Our failure to find at most points the T^3 and E^3 scattering rate dependence which ought to arise as a consequence of our model is the most striking feature of the results presented. Although the cube law does not necessarily apply for all electron states in a polyvalent metal, we found a much more rapid rise even in free-electron-like regions, and in any case, Doezema and Wegehaupt (1975) have observed the T^3 law to be valid experimentally at 3 fairly representative points.

At 5°K, the thermal energy k_BT is equivalent to a little more than 100 GHz, which is the spacing in frequency of the points at which α^2F is tabulated. The thermal factors in (3.22) effectively limit to the first 5 or 6 bins the portion of α^2F which is significant in the scattering rate at this temperature. Leung's (1974) calculation was not designed specifically for accuracy in the low frequency regions of $\alpha^2_{\underline{k}}(\omega)F_{\underline{k}}(\omega)$, where a relatively small number of phonons contribute. To perform the integral over $\underline{k}'$ in the definition (2.26) he used a 2°×2° mesh of points; there is a direct trade-off between the fineness of the mesh and the computer time required. For a typical position on the 1/48'th, this would correspond to a rectangle of about $k_F/30$ by $k_F/50$. Taking into account the shape of phonon dispersion curves in general, we estimate the frequency of the first normal-process phonon contributing to the sum to be roughly 1/25 of the maximum phonon frequency; that is, it will fall into the 4th bin or thereabouts. There are, of course, umklapp processes and coupling to transverse phonons at lower frequencies, but a graininess on about this scale should be expected if only small regions of the $\underline{k}'$ sum contribute at low frequencies. In fact, many of the tabulated distributions are zero in the first bin.

While the remarks do not reflect on the accuracy of these distributions for calculating parameters, such as λ, which are affected by phonons of a broad range of frequencies, they probably identify the reasons for the undesirable behaviour of the scattering rate. The agreement (within a factor of 2) of the actual value of $1/\tau$ with experimental measurements seems reasonable in light of this. It is likely that improved values would result if a much finer mesh could be used for the $\underline{k}'$ integration in calculating α^2F, at least for those regions which contribute low-frequency phonons. To use a very fine mesh over the entire Fermi surface would result in a large and unnecessary increase in computer time.

As we have mentioned, the calculation of $\lambda_{\underline{k}}(T)$ is largely immune to inaccuracies in the low-frequency part of the distributions, and our results ought to be good. We know of no experimental determination of $\lambda_{\underline{k}}$ at elevated temperatures in Al, although such measurements have been performed on other materials using cyclotron resonance (Goy and Castaing, 1973; Sabo, 1969). The surface-Landau-level technique, which avoids the more or less undesirable orbital averages of other magnetic resonance methods, has been used by Doezema and Wegehaupt (1975) to obtain $\lambda_{\underline{k}}$ in aluminum at low temperatures, and could give measurements at higher T. It is evident from figure 3 that temperatures on the order of 50° would be needed to observe the anisotropy in $\lambda_{\underline{k}}(T)/\lambda_{\underline{k}}(0)$, although at 30° a more or less isotropic 4.5% increase in λ should be visible. A higher microwave frequency than the 36 GHz used by Doezema and Wegehaupt to measure scattering rates at 20°K would be necessary, from the requirement that the microwave energy be larger than the $\hbar/\tau$ broadening of the energy levels. From the present calculations, the lifetime broadening at 50°K would correspond to a frequency of about 40 to 200 GHz. Doezema and Koch (1975) report that the resonances disappear at 2000-3000 GHz due to a vanishing of the transition matrix element, an effect which would likely be enhanced at higher temperatures by the rapid increase of the resistivity and resulting increase in skin depth. There would not necessarily be sufficient resolution to observe the anisotropy seen in our calculations.

The energy dependence of $\tau_{\underline{k}}$ may be observed by varying the exciting frequency or by observing higher-order transitions (Gantmakher, 1972). However, it is connected closely to the temperature dependence and may not be of much additional interest.

REFERENCES

Allen, P.B. and Cohen, M.L., 1969, Phys. Rev. *B1*, 1329.

Animalu, A.O.E. and Heine, V., 1965, Phil. Mag. *12*, 1249.

Ashcroft, N.W., 1963, Phil. Mag. *8*, 2055.

Brockhouse, B.N., Hallman, E.D. and Ng, S.C., 1968, in *Magnetic and Inelastic Scattering of Neutrons by Metals*, ed. T. J. Rowland and P. A. Beck, Gordon and Breach, New York.

Doezema, R.E. and Koch, J.F., 1975, Phys. Cond. Matter *19*, 17.

Doezema, R.E. and Wegehaupt, T., 1975, Solid State Commun. *17*, 631.

Fetter, A.L. and Walecka, J.D. 1971, *Quantum Theory of Many-Particle Systems*, McGraw-Hill, Toronto.

Gantmakher, V.F., 1974, Rep. Prog. Phys. *37*, 317.

Goy, P. and Castaing, B., 1973, Phys. Rev. *B7*, 4409.

Grimvall, G., 1968, J. Phys. Chem. Solids *29*, 1221.

Harrison, W.A., 1966, *Pseudopotentials in the Theory of Metals*, W.A. Benjamin, Inc., New York.

Heine, V. and Abarenkov, I., 1964, Phil. Mag. *9*, 451.

Herring, C., 1940, Phys. Rev. *57*, 1169.

Leavens, C.R. and Carbotte, J.P., 1971, Solid State Commun. *9*, 75.

Leung, H.K., 1974, Ph.D. Thesis, McMaster University, Hamilton, Canada.

Maradudin, A.A., 1969, in *Elementary Excitations in Solids*, ed. A.A. Maradudin and G.F. Nardelli, Plenum Press, New York.

Pathria, R.K., 1972, Statistical Mechanics, Pergamon Press, Toronto.

Sabo, J.J., Jr., 1969, Phys. Rev. B1, 1325.

Scalapino, D.J., 1969, in Superconductivity, ed. R. D. Parks, Marcel Dekker Inc., New York.

Tomlinson, P.G. and Carbotte, J.P., 1976, Solid State Commun. 18, 119.

White, B.A., 1974, M.Sc. Thesis, McMaster University, Hamilton, Canada.

Wilkins, J.W., 1968, Observable Many-Body Effects in Metals, NORDITA, Copenhagen.

Ziman, J.M., 1960, Electrons and Phonons, Oxford University Press, London.

Ziman, J.M., 1972, Principles in the Theory of Solids, Cambridge University Press, London.